

CP violation: Dalitz interference, CPT and FSI

J. H. Alvarenga Nogueira^a, I. Bediaga^b, A. B. R. Cavalcante^b, T. Frederico^a, O. Lourenço^c

^a*Instituto Tecnológico de Aeronáutica, DCTA, 12228-900, São José dos Campos, SP, Brazil*

^b*Centro Brasileiro de Pesquisas Físicas, 22290-180, Rio de Janeiro, RJ, Brazil*

^c*Departamento de Ciências da Natureza, Matemática e Educação, CCA, Universidade Federal de São Carlos, 13600-970, Araras, SP, Brazil*

(Dated: March 5, 2022)

Resonances and final state interactions (FSI) play a role in the formation of CP violation (CPV) constrained by CPT invariance. We provide a general formulation of CPV including resonances and FSI starting from the CPT constraint. Our discussion is elaborated within a simple B decay model with the ρ and $f_0(980)$ resonances plus a non resonant background including the $\pi\pi \rightarrow KK$ coupled amplitude. We consider few illustrative examples to show the interference patterns appearing in the CP asymmetry, namely, that from the ρ resonance plus a non-resonant amplitude, and that from the interference of the ρ and $f_0(980)$ resonances. We perform the fit of the CP asymmetry for the charmless three-body B^\pm decay channel $B^\pm \rightarrow \pi^\pm \pi^+ \pi^-$ and obtain as outcome the $B^\pm \rightarrow \pi^\pm K^+ K^-$ for $\pi\pi$ channel asymmetry in the mass region below 1.6 GeV in fair agreement with the new data LHCb data. Analogously, we also describe the CP asymmetry of the $B^\pm \rightarrow K^\pm \pi^+ \pi^-$ decay, with that from the $B^\pm \rightarrow K^\pm K^+ K^-$ channel obtained as output. As in the previous case, we also found agreement with LHCb experimental data.

PACS numbers: 13.25.Hw, 11.30.Er, 11.80.Gw, 12.15.Hh

I. INTRODUCTION

The exact CPT invariance implies the identity of the lifetime of a particle and its charge conjugate. Therefore, when the individual partial decay widths of CP conjugate channels are different, due to the CP violation (CPV), the other channels must have equal amount of CP violation, with opposite sign, such that the total width of the particle and antiparticle are equal. Final state interaction must be the responsible to distribute the CP asymmetry among the different conjugate decay channels such as the sum of partial widths provides identical total width for the particle and its anti-particle.

The common belief says that CPT invariance is not a practical constraint to be taken into account when computing CP violation in charmless B decays. It is naively expected that CP violation is distributed among several different coupled final state channels with two, three, four and more hadrons [1]. Therefore, the CPT constraint should be realized, in principle, by summing up over many hadronic decay channels. However, since hadronic many-body rescattering effects are far from being understood, it is evident that this phenomenological hypothesis should be better understood before consider its important consequences for the description of the CP violation phenomena.

In an opposite direction to the common believe, we shown in detail in a previous paper [2], that the coupling between several final states must be suppressed at least in some charmless three body B decays. A quick observation to the event distribution of these decays shows that they are placed basically at the boundary of the Dalitz plot, in a region dominated by light two-body resonances. This dominance can be directly associated with the non-perturbative regime at the B mass energy [3]. In

addition, by considering the observations made by early experiments [4, 5] that the low mass $\pi\pi$ and $K\pi$ region is dominated by the elastic regime, the number of coupled channel expected for charmless three-body B decays should be very restricted. There is a significant exception to this general picture for the two-body mass distribution: the S-wave $\pi\pi \rightarrow KK$ re-scattering process between 1 to 1.6 GeV [6, 7], that was also discussed in detail in our previous paper. So, at least for this class of decays, the existence of few possibilities of coupled hadronic channels demands the explicit consideration of the important constraint from CPT invariance in the study of CP violation. Unfortunately little is known, either theoretically or experimentally, about the event distribution for others coupled channels with four or more hadrons in the final state. However, by looking at the profusion of observed low mass vector-vector charmless B decays, it seems that they are also dominated by low mass resonances [8].

The inclusive CP asymmetry recently released by the LHCb collaboration for four charged B charmless three-body decays, gives a hint about the correlation among the asymmetries in the coupled decay channels [9]. Actually, the experimental results for strangeness $\Delta = 1$ decays $A_{CP}(B^\pm \rightarrow K^\pm \pi^+ \pi^-) = +0.025 \pm 0.004 \pm 0.004 \pm 0.007$ and $A_{CP}(B^\pm \rightarrow K^\pm K^+ K^-) = -0.036 \pm 0.004 \pm 0.002 \pm 0.007$ multiplied by the observed number of events [9] and corrected by the branching fractions (see Ref. [8]), which represent approximately the efficiency not reported in the paper, show that the number of events involved in the CP asymmetry in one decay channel is approximately the same in the other channel but with opposite sign. The same happens, within the experimental errors, to the coupled decay channels with strangeness $\Delta = 0$. Taking into account the experimental values $A_{CP}(B^\pm \rightarrow \pi^\pm \pi^+ \pi^-) = +0.058 \pm 0.008 \pm 0.009 \pm 0.007$

and $A_{CP}(B^\pm \rightarrow \pi^\pm K^+ K^-) = -0.123 \pm 0.017 \pm 0.012 \pm 0.007$, the number of events observed in each channel, corrected in the same way as before by the branching fractions, show the same correlation as above, namely, a similar number of events involved in the CP asymmetry but with opposite signs.

Beyond the inclusive CPV, three-body decays allow to observe this asymmetry in the Dalitz phase-space. In principle, we can expect CP violation in charmless three-body B decays coming from three different types of interferences involving weak and strong phases: (i) direct CPV due to the interference of the tree and penguin amplitudes in the same intermediate state. This first kind of CPV is based in the BSS model [10]. (ii) CP asymmetry produced through the interference between two different final states with different weak phases coupled by the final state interaction. This second case is constrained by the CPT invariance and it was already well described in our previous work [2]. (iii) CPV from the interference between two neighbor resonances in the Dalitz plot, which share the same-phase space region. This third CPV kind has been pointed out in previous theoretical papers [11–16].

The present study addresses the three types of dynamics related with CPV in the Dalitz plot discussed above and, more specifically, we look for signatures involving each one of these contributions in the charmless decay channels $B^\pm \rightarrow \pi^\pm \pi^+ \pi^-$, $B^\pm \rightarrow \pi^\pm K^+ K^-$, $B^\pm \rightarrow K^\pm \pi^+ \pi^-$ and $B^\pm \rightarrow K^\pm K^+ K^-$. To perform this study, we use the recently published LHCb paper [9], in particular, the $\pi^+ \pi^-$ and $K^+ K^-$ mass distribution from the difference between B^- and B^+ . These differences other than give directly the CP violation distribution in the phase-space, minimize substantially problems of acceptance and background not available in the LHCb paper.

Our work develops a CP asymmetry formula including resonances and FSI based on the CPT constraint. The CP asymmetry is derived in lowest order in the strong interaction and decomposed in angular momentum. The explicit expression for the CP asymmetry is found for the decays channels $B^\pm \rightarrow \pi^\pm \pi^+ \pi^-$ and $B^\pm \rightarrow K^\pm \pi^+ \pi^-$. Our discussion is exemplified by considering, within the isobar model, the interference patterns for the CP asymmetry from the ρ and $f_0(980)$ resonances plus a non resonant background including the contribution of the $\pi\pi \rightarrow KK$ coupled channel amplitude. We use this formula to fit the recent $B^\pm \rightarrow \pi^\pm \pi^+ \pi^-$ LHCb data [9] and obtain as outcome the $B^\pm \rightarrow \pi^\pm K^+ K^-$ in qualitative agreement with data for the mass region below 1.6 GeV. We apply the same procedure to the $B^\pm \rightarrow K^\pm \pi^+ \pi^-$ and $B^\pm \rightarrow K^\pm K^+ K^-$ decays. We also take into account the LHCb separation between positive and negative $\cos\theta$ values, that supplies new details which reveal the role of the vector meson resonance in building the CP asymmetry interference pattern.

The work is organized as follows. A brief review of the CPT constraint for deriving the CP asymmetry with

FSI and our notation are provided in Sec. II. The CP asymmetry formula in leading order of the strong interaction and angular momentum decomposition is given in Sec. III. The resonances are introduced in the CP asymmetry expression in Sec. IV. The formula for the interfering resonant and non-resonant amplitudes in the asymmetry is developed in Sec. V. The analysis of the various CP asymmetry terms is given in Sec. VI. The results from the fitting procedure to the asymmetry in the $B^\pm \rightarrow \pi^\pm \pi^+ \pi^-$ are shown in Sec. VII, where we found that the CPT violating terms can be disregarded. We also show results for $B^\pm \rightarrow \pi^\pm K^+ K^-$ decay with no new parameters. An analogous study is performed at Sec. VIII for $B^\pm \rightarrow K^\pm \pi^+ \pi^-$ and $B^\pm \rightarrow K^\pm K^+ K^-$ decays. The concluding remarks are provided in Sec. IX, where we also discuss a more general formula to the CP asymmetry, where the FSI terms interfere with the ρ and $f_0(980)$ resonances. In the Appendices, we show the angle integrated asymmetry as well as the derivation of kinematical factors.

II. CPT INVARIANCE IN A WEAK DECAY

We follow closely Refs. [2, 17, 18] to introduce our notation and the CPT constraint in B meson decays. We start by reminding that the weak and strong Hamiltonians conserve CPT, namely,

$$(CPT)^{-1} H_w (H_s) CPT = H_w (H_s) . \quad (1)$$

The hadron weak decay amplitude is computed from the matrix element $\langle \lambda_{out} | H_w | h \rangle$, where the distorted state λ_{out} has the effect of the hadronic strong force due to FSI. The requirement of CPT invariance on the decay amplitude is

$$\langle \lambda_{out} | H_w | h \rangle = \chi_h \chi_\lambda \langle \bar{\lambda}_{in} | H_w | \bar{h} \rangle^* , \quad (2)$$

where we used that the hadron state $|h\rangle$ transforms under CPT as $CPT |h\rangle = \chi(\bar{h})$, where \bar{h} is the charge conjugate state and χ a phase.

The completeness relation of the strongly interacting states, eigenstates of H_s , and the hermiticity of H_w implies that

$$\langle \lambda_{out} | H_w | h \rangle = \chi_h \chi_\lambda \sum_{\bar{\lambda}'} S_{\bar{\lambda}', \bar{\lambda}} \langle \bar{\lambda}'_{out} | H_w | \bar{h} \rangle^* , \quad (3)$$

where

$$S_{\bar{\lambda}', \bar{\lambda}} = \langle \bar{\lambda}'_{out} | \bar{\lambda}_{in} \rangle = S_{\lambda', \lambda} \quad (4)$$

defines the matrix elements of the S-matrix. The sum of the partial widths of the hadron decay channels and the correspondent sum for the charge conjugate are identical, i.e. the mean life of the particle and its conjugate are equal, which is a consequence of Eq. (3) and the hermiticity of H_w (see Ref. [2]):

$$\sum_\lambda |\langle \lambda_{out} | H_w | h \rangle|^2 = \sum_{\bar{\lambda}} |\langle \bar{\lambda}_{out} | H_w | \bar{h} \rangle|^2 . \quad (5)$$

The CP-violating phase enters linearly at lowest order in the hadron decay amplitude as suggested by the BSS mechanism [10]. In general, the decay amplitude can be written as

$$\mathcal{A}^\pm = A_\lambda + B_\lambda e^{\pm i\gamma}, \quad (6)$$

where A_λ and B_λ are complex amplitudes invariant under CP, containing the strongly interacting final-state channel, i.e.,

$$\mathcal{A}^- = \langle \lambda_{out} | H_w | h \rangle, \quad (7)$$

and

$$\mathcal{A}^+ = \langle \bar{\lambda}_{out} | H_w | \bar{h} \rangle. \quad (8)$$

The only change due to the CP transformation is the sign multiplying the weak phase γ . The CPT condition depicted by Eq. (5) gives

$$\sum_\lambda \Gamma(A_\lambda^-) = \sum_{\bar{\lambda}} \Gamma(A_{\bar{\lambda}}^+), \quad (9)$$

where the subindex labels the final state channels, summed up in the kinematically allowed phase-space. The decay amplitude written in terms of the CPT constraint (3), and considering the CP violating amplitudes for the hadron and its charge conjugate is

$$A_\lambda + e^{\mp i\gamma} B_\lambda = \chi_h \chi_\lambda \sum_{\lambda'} S_{\lambda',\lambda} (A_{\lambda'} + e^{\pm i\gamma} B_{\lambda'})^* \quad (10)$$

Note that this equation imposes a relation between A_λ or B_λ with their respective complex conjugates.

III. CP ASYMMETRY AND FSI IN LEADING ORDER

The S-matrix is given in terms of the scattering amplitude $t_{\lambda',\lambda}$, namely,

$$S_{\lambda',\lambda} = \delta_{\lambda',\lambda} + i t_{\lambda',\lambda}, \quad (11)$$

which turns Eq. (10) into

$$A_\lambda + e^{\mp i\gamma} B_\lambda = \chi_h \chi_\lambda (A_\lambda + e^{\pm i\gamma} B_\lambda)^* + i \chi_h \chi_\lambda \sum_{\lambda'} t_{\lambda',\lambda} (A_{\lambda'} + e^{\pm i\gamma} B_{\lambda'})^*. \quad (12)$$

We now consider effect of the FSI in leading order in the decay amplitudes A_λ and B_λ . For that purpose, let us introduce decay amplitudes computed without the effect of the final state interaction,

$$\langle \lambda_0 | H_w | h \rangle = A_{0\lambda} + e^{-i\gamma} B_{0\lambda}, \quad (13)$$

and

$$\langle \bar{\lambda}_0 | H_w | \bar{h} \rangle = A_{0\lambda} + e^{+i\gamma} B_{0\lambda}, \quad (14)$$

where $|\lambda_0\rangle$ and $|\bar{\lambda}_0\rangle$ are the mesonic noninteracting charge conjugate states, i.e., without the distortion of

the strong hadronic interaction. The terms $A_{0\lambda}$ and $B_{0\lambda}$ can be in principle associated with the tree and penguin amplitudes in the BSS model [10].

The leading order (LO) effect due to FSI in the decay amplitude is obtained by substituting $A_\lambda \rightarrow A_{0\lambda}$ and $B_\lambda \rightarrow B_{0\lambda}$ in the right-hand side of Eq. (12). Considering, the assumption of the CPT invariance of the weak Hamiltonian one has also that:

$$\langle \lambda_0 | H_w | h \rangle = \chi_h \chi_\lambda \langle \bar{\lambda}_0 | H_w | \bar{h} \rangle^*, \quad (15)$$

which implies in the following relation for the partonic amplitudes

$$A_{0\lambda} = \chi_h \chi_\lambda A_{0\lambda}^* \quad (16)$$

and

$$B_{0\lambda} = \chi_h \chi_\lambda B_{0\lambda}^*, \quad (17)$$

and therefore up to the leading order in $t_{\lambda',\lambda}$, Eq. (12) reduces to

$$\begin{aligned} \mathcal{A}_{LO}^\pm &= A_{0\lambda} + e^{\pm i\gamma} B_{0\lambda} \\ &+ i \sum_{\lambda'} t_{\lambda',\lambda} (A_{0\lambda'} + e^{\pm i\gamma} B_{0\lambda'}), \end{aligned} \quad (18)$$

which is equivalent to the one provided in Refs. [19, 20].

In lowest order the scattering amplitude is restricted only to two-body terms, therefore it is useful to decompose the source decay amplitudes $A_{0\lambda}$, $B_{0\lambda}$ and the $t_{\lambda',\lambda}$ matrix in angular momentum states J of each pair in the outgoing channel. The angular momentum decomposition will allow to identify and introduce the meson resonances, like the $\rho(770)$ or $f_0(980)$ in the $\pi\pi$ channel. This leading order decay amplitude (18) decomposed in J is written as,

$$\begin{aligned} \mathcal{A}_{LO}^\pm &= \sum_J (A_{0\lambda}^J + e^{\pm i\gamma} B_{0\lambda}^J) \\ &+ i \sum_{\lambda', J} t_{\lambda',\lambda}^J (A_{0\lambda'}^J + e^{\pm i\gamma} B_{0\lambda'}^J), \end{aligned} \quad (19)$$

where one should note that $\lambda(\lambda')$ refers to two-body channels in the final hadronic state including all other dependences on the quantum numbers and in the energy-momentum of the spectator hadrons. By using this expression, the CP asymmetry can be written as

$$\begin{aligned} \Delta\Gamma_\lambda &= \Gamma(h \rightarrow \lambda) - \Gamma(\bar{h} \rightarrow \bar{\lambda}) \\ &= 4(\sin \gamma) \sum_{J J'} \text{Im} \left\{ (B_{0\lambda}^J)^* A_{0\lambda}^{J'} \right. \\ &\quad \left. + i \sum_{\lambda'} \left[(B_{0\lambda}^J)^* t_{\lambda',\lambda}^{J'} A_{0\lambda'}^{J'} - (B_{0\lambda'}^{J'} t_{\lambda',\lambda}^{J'})^* A_{0\lambda}^J \right] \right\}, \end{aligned} \quad (20)$$

where the λ' represents each state coupled by the strong interaction to the decay channel λ . We just remind that the second and third terms in the right-hand side of Eq. (20) can be associated to the ‘‘compound’’ CP asymmetry [21]. These two terms cancel each other when

summed in all channels λ and integrated over the phase-space, that leads to the CPT condition expressed by Eq. (9), once the source term in (20) satisfies

$$\sum_{\lambda J} \text{Im} \left[(B_{0\lambda}^J)^* A_{0\lambda}^J \right] = 0, \quad (21)$$

which is a consequence of the CPT constraint at the microscopic level, e.g., as expressed by the tree and penguin amplitudes in the BSS model, that should be valid when FSI is turned off in Eq. (2). This term was neglected by Wolfenstein, which corresponds to the trivial solution of Eq. (21), assuming that the phase difference between the two CP-conserving amplitudes is zero for all decay channels.

To be complete and detailing the notation of Ref. [2] by including the two-particle angular momentum states J , we show that the second term in Eq. (20),

$$\begin{aligned} \sum_{\lambda} \Delta \Gamma_{\lambda}^{FSI} &= 4(\sin \gamma) \sum_{\lambda \lambda' J} \text{Re} \left[(B_{0\lambda}^J)^* t_{\lambda', \lambda}^J A_{0\lambda'}^J \right. \\ &\quad \left. - (B_{0\lambda}^J t_{\lambda, \lambda'}^J)^* A_{0\lambda}^J \right], \end{aligned} \quad (22)$$

also satisfies the CPT condition, namely, this quantity vanishes, which is easily verified by using Eqs. (17) as

$$\begin{aligned} \sum_{\lambda} \Delta \Gamma_{\lambda}^{FSI} &= 4(\sin \gamma) \times \\ &\times \sum_{\lambda' \lambda J} \text{Re} \left[\chi_h \chi_{\lambda J} (B_{0\lambda}^J)^* t_{\lambda', \lambda}^J (A_{0\lambda'}^J)^* \right. \\ &\quad \left. - \chi_h^* \chi_{\lambda' J}^* B_{0\lambda'}^J (t_{\lambda', \lambda}^J)^* A_{0\lambda}^J \right] = 0. \end{aligned} \quad (23)$$

The vanishing of Eq. (23) is due to the symmetry of $t_{\lambda, \lambda'}^J = t_{\lambda', \lambda}^J$, and the fact that $\chi_{\lambda J} = \chi_{\lambda' J}$, i.e., the strong interaction does not mix different CP eigenstates. Therefore, by taking into account Eqs. (21) and (23), one has that the CPT constraint

$$\begin{aligned} \sum_{\lambda} \Delta \Gamma_{\lambda} &= 4(\sin \gamma) \sum_{\lambda J} \text{Im} \left[(B_{0\lambda}^J)^* A_{0\lambda}^J \right] \\ &\quad + \sum_{\lambda} \Delta \Gamma_{\lambda}^{FSI} = 0, \end{aligned} \quad (24)$$

is fulfilled in leading order of the interaction.

IV. RESONANT CHANNELS AND CPT

In the case that the channel λ contains also the formation of a resonance in the partonic process, namely,

$B \rightarrow \pi \rho$, the amplitudes $A_{0\lambda}$ and $B_{0\lambda}$ can be separated in the following two parts, $A_{0\lambda}^J = A_{0\lambda NR}^J + \sum_R A_{0\lambda R}^J$, and $B_{0\lambda}^J = B_{0\lambda NR}^J + \sum_R B_{0\lambda R}^J$, where the subindex R and NR mean resonant and non resonant channels. Therefore, the decay amplitude in Eq. (19) is rewritten as

$$\begin{aligned} \mathcal{A}_{LO}^{\pm} &= \sum_J \left[\sum_R A_{0\lambda R}^J + A_{0\lambda NR}^J + \right. \\ &\quad \left. + e^{\pm i\gamma} \left(\sum_R B_{0\lambda R}^J + B_{0\lambda NR}^J \right) \right] \\ &\quad + i \sum_{\lambda', J} t_{\lambda', \lambda}^J \left[\sum_R A_{0\lambda' R}^J + A_{0\lambda' NR}^J \right. \\ &\quad \left. + e^{\pm i\gamma} \left(\sum_R B_{0\lambda' R}^J + B_{0\lambda' NR}^J \right) \right]. \end{aligned} \quad (25)$$

The resonant source terms $A_{0\lambda R}^J$ and $B_{0\lambda R}^J$ should be interpreted as bare amplitudes, where at the resonance decay vertex, the two-hadron rescattering process is not yet included. The Breit-Wigner amplitudes for each term are identified according to

$$(1 + i t_{\lambda\lambda}^J) A_{0\lambda R}^J \rightarrow a_0^R F_{R\lambda}^{BW} P_J(\cos \theta) \quad (26)$$

and

$$(1 + i t_{\lambda\lambda}^J) B_{0\lambda R}^J \rightarrow b_0^R F_{R\lambda}^{BW} P_J(\cos \theta), \quad (27)$$

where J is the spin of the resonance decaying to two spin zero particles and $P_J(\cos \theta)$ is the Legendre polynomial and θ is the helicity angle between the equally charge particles in the Gottfried-Jackson frame. We will give the representation of this angle for the $B^+ \rightarrow \pi^+ \pi^+ \pi^-$ decay in Fig. 1 of the next section.

After substituting (27) in (25), we get that

$$\begin{aligned} \mathcal{A}_{LO}^{\pm} &= \sum_{JR} (a_{0\lambda}^R + e^{\pm i\gamma} b_0^R) F_{R\lambda}^{BW} P_J(\cos \theta) \\ &\quad + \sum_J (A_{0\lambda NR}^J + e^{\pm i\gamma} B_{0\lambda NR}^J) \\ &\quad + i \sum_{\lambda', J} t_{\lambda', \lambda}^J (A_{0\lambda' NR}^J + e^{\pm i\gamma} B_{0\lambda' NR}^J), \end{aligned} \quad (28)$$

where the first and second terms in the right-hand side is the isobar model for the decay. The second term is the source term for the final state channel, and the third one includes the hadronic interaction among the two of the hadrons with angular momentum J . We should clarify that Eq. (28) includes the interaction in the resonance region as the pair of hadrons has a probability to be formed directly from the partonic process.

The CP asymmetry from Eq. (28) can be cast in the following form

$$\begin{aligned}\Delta\Gamma_\lambda &= \Gamma(h \rightarrow \lambda) - \Gamma(\bar{h} \rightarrow \bar{\lambda}) \\ &= 4(\sin \gamma) \sum_{JJ'} \text{Im} \left\{ \left(\sum_R b_{0\lambda}^R F_{R\lambda}^{BW} P_J(\cos \theta) + B_{0\lambda NR}^J \right)^* \left(\sum_{R'} a_{0\lambda}^{R'} F_{R'\lambda}^{BW} P_{J'}(\cos \theta) + A_{0\lambda NR}^{J'} \right) \right. \\ &\quad + i \sum_{\lambda'} \left(\sum_R b_{0\lambda}^R F_{R\lambda}^{BW} P_J(\cos \theta) + B_{0\lambda NR}^J \right)^* t_{\lambda',\lambda}^{J',\lambda} \left(\sum_{R'} a_{0\lambda'}^{R'} F_{R'\lambda'}^{BW} P_{J'}(\cos \theta) + A_{0\lambda' NR}^{J'} \right) \\ &\quad \left. - i \sum_{\lambda'} \left(\sum_{R'} b_{0\lambda'}^{R'} F_{R'\lambda'}^{BW} P_{J'}(\cos \theta) + B_{0\lambda' NR}^{J'} \right)^* [t_{\lambda',\lambda}^{J',\lambda}]^* \left(\sum_R a_{0\lambda}^R F_{R\lambda}^{BW} P_J(\cos \theta) + A_{0\lambda NR}^J \right) \right\}. \quad (29)\end{aligned}$$

It has to be understood that the subindex λ also includes different kinematical regions of the three-body channel. Since we have introduced the Breit-Wigner amplitudes in the decay amplitude, the CPT constraint has to be checked in the actual fit, i.e., if $\sum_\lambda \Delta\Gamma_\lambda = 0$ is satisfied when one takes into account the integration over the phase-space besides the sum over all decay channels in the sum of λ . Indeed, in our fitting procedure, we will keep only terms that, within our limited model, satisfy the CPT constraint.

V. INTERFERING RESONANT AND NON RESONANT AMPLITUDES

We present a simple example to explore the asymmetry formula (29), considering the resonant, non-resonant source terms and the contribution from the coupling between two strongly interacting channels, namely $\pi\pi$ and KK . We use the vector and scalar resonances, the $\rho(770)$ and $f_0(980)$ ones, for instance, interfering with a non resonant amplitude and the term carrying the strong interaction transition amplitude between the coupled channels. This illustrates exactly the $B^\pm \rightarrow \pi^\pm \pi^+ \pi^-$ decay case at low invariant $\pi^+ \pi^-$ mass. Also there are $B^\pm \rightarrow K^\pm \pi^+ \pi^-$ data [22, 23] previous to the CP asymmetry observation by LHCb collaboration.

First, let us remind that, in a general way, the Breit-Wigner excitation curve for a resonance R reads

$$F_R^{BW}(s) = \frac{1}{m_R^2 - s - im_R \Gamma_R(s)}, \quad (30)$$

with m_R being the resonance mass, and

$$\Gamma_R(s) = \frac{\left(\frac{s}{4} - m_\pi^2\right)^{1/2} m_R \Gamma'_R}{\left(\frac{m_R^2}{4} - m_\pi^2\right)^{1/2} s^{1/2}}, \quad (31)$$

denoting the energy dependent relativistic width. For the pion mass, we adopted $m_\pi = 0.138$ GeV, degenerated for the negative and positive charged particles. Here, we consider the resonance decay in the $\pi\pi$ channel.

The real and imaginary parts of $F_R^{BW}(s)$ are given, respectively, by

$$\text{Re}[F_R^{BW}] = \frac{m_R^2 - s}{(m_R^2 - s)^2 + m_R^2 \Gamma_R(s)^2}, \quad (32)$$

and

$$\text{Im}[F_R^{BW}] = \frac{m_R \Gamma_R(s)}{(m_R^2 - s)^2 + m_R^2 \Gamma_R(s)^2}. \quad (33)$$

The square modulus is

$$|F_R^{BW}|^2(s) = \frac{1}{(m_R^2 - s)^2 + m_R^2 \Gamma_R(s)^2}. \quad (34)$$

The amplitudes for $B^\pm \rightarrow \pi^\pm \pi^+ \pi^-$ or $B^\pm \rightarrow K^\pm \pi^+ \pi^-$ decays, taking into account the $\rho(770)$ and $f_0(980)$ resonances interfering with a constant non resonant amplitude, can be written as

$$\begin{aligned}\mathcal{A}_{0\lambda}^\pm &= a_0^\rho F_\rho^{BW} k(s) \cos \theta + a_0^f F_f^{BW} + \frac{a_{0\lambda}^{nr} + b_{0\lambda}^{nr} e^{\pm i\gamma}}{1 + \frac{s}{\Lambda_\lambda^2}} \\ &\quad + [b_0^\rho F_\rho^{BW} k(s) \cos \theta + b_0^f F_f^{BW}] e^{\pm i\gamma}, \quad (35)\end{aligned}$$

where the kinematical factor $k(s) = \sqrt{1 - \frac{4m_\pi^2}{s}}$ is included in the amplitude of the $\rho(770)$ vector resonance, to take into account the threshold behavior of the decay amplitude in a p -wave. The angle θ is defined as the angle between the bachelor and the equally charged interacting particle. See this definition in the $B^+ \rightarrow \pi^+ \pi^+ \pi^-$ decay illustrated in Fig. 1. Here, $\cos \theta$ is associated to the spin 1 of the ρ resonance and varies from -1 to $+1$ along the phase space.

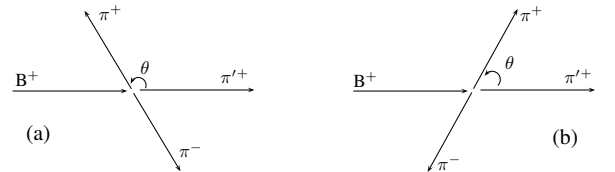


FIG. 1. $B^+ \rightarrow \pi^+ \pi^+ \pi^-$ decay with π^+ being the bachelor particle. (a): $\cos \theta < 0$ ($\theta > \frac{\pi}{2}$). (b): $\cos \theta > 0$ ($\theta < \frac{\pi}{2}$).

The form factor $\left(1 + \frac{s}{\Lambda_\lambda^2}\right)^{-1}$ is included in the non resonant amplitude in order to parametrize the dependence on the square mass of the pair that is brought by the source terms, either for the $\pi\pi$ or KK systems. It comes from the partonic decay amplitude that produces the three-meson final state, in which the relative momentum between the pair of mesons is distributed among the quarks in the momentum loop within the microscopic amplitude, e. g., the tree and penguin diagrams, and probe the internal structure of the mesons involved in the initial and final states. In general, the non resonant amplitude should depend on the two kinematically independent Mandelstam variables, which for simplicity, we choose one of them. The suggestion is that the microscopic process gives raise to the momentum dependence in a power-law form reflecting the hard momentum structure of the mesons involved in the decay [24]. For example, inspecting the tree diagram, one observes that the decay of the b -quark in the rest frame, produces a fast light quark and a pion back to back. The light quark has to share its momentum with a slow antiquark, which is happens by the gluon exchange and is damped by a momentum power-law form. A similar reasoning can be applied to the penguin diagram. On the other hand, if factorization can be proved, the heavy to light generalized transition form factors [25] like a heavy meson into $K\pi/\pi\pi$, for instance, will also play a role in CPV studies.

An alternative to parametrize the decay amplitude,

convenient for Monte-Carlo simulations, is to write Eq. (35) as

$$\mathcal{A}_{0\lambda}^\pm = a_\pm^\rho e^{i\delta_\pm^\rho} F_\rho^{\text{BW}} k(s) \cos\theta + a_\pm^f e^{i\delta_\pm^f} F_f^{\text{BW}} + \frac{a_{\pm\lambda}^{nr} e^{i\delta_{\pm\lambda}^{nr}}}{1 + \frac{s}{\Lambda_\lambda^2}}, \quad (36)$$

where δ_\pm^ρ and δ_\pm^f contain both the fixed weak and strong phases, with the Breit-Wigner functions introducing additional mass dependent strong phases as sketched above. The phase $\delta_{\pm\lambda}^{nr}$ comes from the partonic amplitude producing the three-body final state, excluding the strong phase from the rescattering process. The relation between the parameters is $a_\pm^\rho e^{i\delta_\pm^\rho} = a_0^\rho + b_0^\rho e^{\pm i\gamma}$, $a_\pm^f e^{i\delta_\pm^f} = a_0^f + b_0^f e^{\pm i\gamma}$, and $a_{\pm\lambda}^{nr} e^{i\delta_{\pm\lambda}^{nr}} = a_{0\lambda}^{nr} + b_{0\lambda}^{nr} e^{\pm i\gamma}$.

By comparing the first term in the r.h.s. of Eqs. (29) and (35), it is possible to make the following identifications, namely,

$$\begin{aligned} A_{0\lambda R} &= a_0^\rho F_\rho^{\text{BW}} k(s) \cos\theta + a_0^f F_f^{\text{BW}}, \\ B_{0\lambda R} &= b_0^\rho F_\rho^{\text{BW}} k(s) \cos\theta + b_0^f F_f^{\text{BW}}, \\ A_{0\lambda NR} &= \frac{a_{0\lambda}^{nr}}{1 + \frac{s}{\Lambda_\lambda^2}}, \\ B_{0\lambda NR} &= \frac{b_{0\lambda}^{nr}}{1 + \frac{s}{\Lambda_\lambda^2}}, \end{aligned} \quad (37)$$

and thus, rewrite Eq. (29) for the decay channels $\lambda = \pi\pi\pi$ or $K\pi\pi$ as

$$\begin{aligned} \Delta\Gamma_\lambda &= 4(\sin\gamma)\text{Im}\left[\left(b_0^\rho F_\rho^{\text{BW}} k(s) \cos\theta + b_0^f F_f^{\text{BW}} + \frac{b_{0\lambda}^{nr}}{1 + \frac{s}{\Lambda_\lambda^2}}\right)^* \left(a_0^\rho F_\rho^{\text{BW}} k(s) \cos\theta + a_0^f F_f^{\text{BW}} + \frac{a_{0\lambda}^{nr}}{1 + \frac{s}{\Lambda_\lambda^2}}\right)\right] \\ &+ 4(\sin\gamma)\text{Re}\left\{\sum_{\lambda'}\left[\left(b_0^\rho F_\rho^{\text{BW}} k(s) \cos\theta + b_0^f F_f^{\text{BW}} + \frac{b_{0\lambda}^{nr}}{1 + \frac{s}{\Lambda_\lambda^2}}\right)^* t_{\lambda',\lambda}^{J=0} \frac{a_{0\lambda'}^{nr}}{1 + \frac{s}{\Lambda_{\lambda'}^2}}\right. \right. \\ &\left. \left.- \left(\frac{b_{0\lambda'}^{nr}}{1 + \frac{s}{\Lambda_{\lambda'}^2}} t_{\lambda',\lambda}^{J=0}\right)^* \left(a_0^\rho F_\rho^{\text{BW}} k(s) \cos\theta + a_0^f F_f^{\text{BW}} + \frac{a_{0\lambda}^{nr}}{1 + \frac{s}{\Lambda_\lambda^2}}\right)\right]\right\}, \end{aligned} \quad (38)$$

where we used the identity $\text{Im}(iz) = \text{Re}(z)$ and kept only one term in the scattering amplitude for $J = 0$ in Eq. (29). The subindex λ are associated with a position in the phase-space of the B decay and λ' is equal to πKK or KKK , in the case of $B \rightarrow \pi\pi\pi$ and $B \rightarrow K\pi\pi$, respectively. The second term in the r.h.s. of Eq. (38) is the compound contribution to the CP asymmetry that includes the effect of the final state interaction in the non resonant channel. In this example, only the S -wave amplitude $KK \rightarrow \pi\pi$ channel was included and we have considered the interference of this term with the resonant ones. We use here the functional form of this term obtained in Ref. [2].

A. CP asymmetry formula

The compound contribution to CPV, namely, the one carrying $t_{\lambda',\lambda}^{J=0}$ in Eq. (38), has as input in our calculations the non-diagonal scattering amplitude depicted in the full S -matrix in the isoscalar and angular momentum zero $\pi\pi \rightarrow KK$ coupled channels, which is written as

$$S = \begin{bmatrix} \eta e^{2i\delta_{\pi\pi}} & i\sqrt{1-\eta^2} e^{i(\delta_{\pi\pi}+\delta_{KK})} \\ i\sqrt{1-\eta^2} e^{i(\delta_{\pi\pi}+\delta_{KK})} & \eta e^{2i\delta_{KK}} \end{bmatrix} \quad (39)$$

with the inelasticity parameter $\eta(s)$ and the $\pi\pi$ phase-shift $\delta_{\pi\pi}(s)$, given by [26],

$$\eta(s) = 1 - \left(\epsilon_1 \frac{k_2}{s^{1/2}} + \epsilon_2 \frac{k_2^2}{s} \right) \frac{M'^2 - s}{s}, \quad (40)$$

with

$$k_2 = \frac{\sqrt{s - 4m_K^2}}{2}, \quad (41)$$

and

$$\delta_{\pi\pi}(s) = \frac{1}{2} \cos^{-1} \left\{ \frac{\cot^2[\delta_{\pi\pi}(s)] - 1}{\cot^2[\delta_{\pi\pi}(s)] + 1} \right\}, \quad (42)$$

with

$$\cot(\delta_{\pi\pi}) = c_0 \frac{(s - M_s^2)(M_f^2 - s)}{M_f^2 s^{1/2}} \frac{|k_2|}{k_2^2}, \quad (43)$$

respectively. In these expressions, we use $m_K = 0.494$ GeV, $M' = 1.5$ GeV, $M_s = 0.92$ GeV, $M_f = 1.32$ GeV, $\epsilon_1 = 2.4$, $\epsilon_2 = -5.5$, and $c_0 = 1.3$, according to the parametrization given in Ref. [26]. The off-diagonal term in the S-matrix gives the transition amplitude between the $\pi\pi$ and KK channels in the isoscalar channel, namely, $t_{\lambda',\lambda}^{J=0} = \sqrt{1 - \eta^2} e^{i(\delta_{\pi\pi} + \delta_{KK})} \approx \sqrt{1 - \eta^2} e^{2i\delta_{\pi\pi}}$, where we have made the approximation $\delta_{KK} \approx \delta_{\pi\pi}$ between 1 and 1.6 GeV.

The expression for the CP asymmetry in Eq. (38), should be expanded in a form where the unknown parameters are exposed in a simple manner to proceed with the fitting to the experimental data. By using the relations $\text{Im}(z_1 z + z_2 z^*) = \text{Re}(z)\text{Im}(z_1 + z_2) + \text{Im}(z)\text{Re}(z_1 - z_2)$, $\text{Re}(z_1^* z_2) = \text{Re}(z_1)\text{Re}(z_2) + \text{Im}(z_1)\text{Im}(z_2)$, and $\text{Im}(z_1^* z_2) = \text{Re}(z_1)\text{Im}(z_2) - \text{Im}(z_1)\text{Re}(z_2)$, together with Eqs. (33)-(34), one can finally write Eq. (38) as

$$\begin{aligned} \Delta\Gamma_\lambda = & \frac{\mathcal{A}}{\left(1 + \frac{s}{\Lambda_\lambda^2}\right)^2} + \frac{\{\mathcal{B} \cos[2\delta_{\pi\pi}(s)] + \mathcal{B}' \sin[2\delta_{\pi\pi}(s)]\} \sqrt{1 - \eta^2(s)}}{\left(1 + \frac{s}{\Lambda_\lambda^2}\right) \left(1 + \frac{s}{\Lambda_{\lambda'}^2}\right)} + \mathcal{C} |F_\rho^{\text{BW}}(s)|^2 k^2(s) \cos^2 \theta \\ & + |F_\rho^{\text{BW}}(s)|^2 k(s) \cos \theta \left\{ \frac{\mathcal{D}(m_\rho^2 - s)}{1 + \frac{s}{\Lambda_\lambda^2}} + \frac{\mathcal{D}' \sqrt{1 - \eta^2(s)} \{m_\rho \Gamma_\rho(s) \cos[2\delta_{\pi\pi}(s)] - (m_\rho^2 - s) \sin[2\delta_{\pi\pi}(s)]\}}{1 + \frac{s}{\Lambda_{\lambda'}^2}} \right. \\ & + \frac{\mathcal{E} m_\rho \Gamma_\rho(s)}{1 + \frac{s}{\Lambda_\lambda^2}} + \frac{\mathcal{E}' \sqrt{1 - \eta^2(s)} \{(m_\rho^2 - s) \cos[2\delta_{\pi\pi}(s)] + m_\rho \Gamma_\rho(s) \sin[2\delta_{\pi\pi}(s)]\}}{1 + \frac{s}{\Lambda_{\lambda'}^2}} \left. \right\} \\ & + |F_\rho^{\text{BW}}(s)|^2 |F_f^{\text{BW}}(s)|^2 k(s) \cos \theta \times \\ & \times \{ \mathcal{F}[(m_\rho^2 - s)(m_f^2 - s) + m_\rho \Gamma_\rho(s) m_f \Gamma_f(s)] + \mathcal{G}[(m_\rho^2 - s) m_f \Gamma_f(s) - m_\rho \Gamma_\rho(s)(m_f^2 - s)] \} \\ & + |F_f^{\text{BW}}(s)|^2 \left\{ \frac{\mathcal{H}(m_f^2 - s)}{1 + \frac{s}{\Lambda_\lambda^2}} + \frac{\mathcal{H}' \sqrt{1 - \eta^2(s)} \{m_f \Gamma_f(s) \cos[2\delta_{\pi\pi}(s)] - (m_f^2 - s) \sin[2\delta_{\pi\pi}(s)]\}}{1 + \frac{s}{\Lambda_{\lambda'}^2}} \right. \\ & + \frac{\mathcal{P} m_f \Gamma_f(s)}{1 + \frac{s}{\Lambda_\lambda^2}} + \frac{\mathcal{P}' \sqrt{1 - \eta^2(s)} \{(m_f^2 - s) \cos[2\delta_{\pi\pi}(s)] + m_f \Gamma_f(s) \sin[2\delta_{\pi\pi}(s)]\}}{1 + \frac{s}{\Lambda_{\lambda'}^2}} \left. \right\} + \mathcal{Q} |F_f^{\text{BW}}(s)|^2, \quad (44) \end{aligned}$$

where λ is associated to $\pi^\pm \pi^+ \pi^-$ or $K^\pm \pi^+ \pi^-$, and λ' to $\pi^\pm K^+ K^-$ or $K^\pm K^+ K^-$. The masses of the resonances are $m_\rho = 0.775$ GeV, and $m_f = 0.975$ GeV [8, 27]. The widths used in Eq. (31) for $R = \rho, f$ are $\Gamma'_\rho = 0.150$ GeV and $\Gamma'_f = 0.044$ GeV. The parameters of the model can be written in terms of those in Eqs. (35) or (36) as follows,

$$\mathcal{A} = 4(\sin \gamma) \text{Im} [a_{0\lambda}^{nr} b_{0\lambda}^{nr*}] = (a_{+\lambda}^{nr})^2 - (a_{-\lambda}^{nr})^2, \quad (45)$$

$$\mathcal{B} = 4(\sin \gamma) \text{Re} [a_{0\lambda}^{nr} b_{0\lambda}^{nr*} - a_{0\lambda}^{nr} b_{0\lambda'}^{nr*}], \quad (46)$$

$$\mathcal{B}' = -4(\sin \gamma) \text{Im} [a_{0\lambda}^{nr} b_{0\lambda}^{nr*} + a_{0\lambda}^{nr} b_{0\lambda'}^{nr*}], \quad (47)$$

$$\mathcal{C} = 4(\sin \gamma) \text{Im} [a_{0\lambda}^{\rho} b_0^{\rho*}] = (a_{+}^{\rho})^2 - (a_{-}^{\rho})^2, \quad (48)$$

$$\begin{aligned} \mathcal{D} &= 4(\sin \gamma) \text{Im} [a_{0\lambda}^{\rho} b_{0\lambda}^{nr*} + a_{0\lambda}^{nr} b_0^{\rho*}] \\ &= 2[a_{+}^{\rho} a_{+\lambda}^{nr} \cos(\delta_{+}^{\rho} - \delta_{+\lambda}^{nr}) - a_{-}^{\rho} a_{-\lambda}^{nr} \cos(\delta_{-}^{\rho} - \delta_{-\lambda}^{nr})], \quad (49) \end{aligned}$$

$$\begin{aligned} \mathcal{D}' &= 4(\sin \gamma) \text{Im} [a_{0\lambda}^{\rho} b_{0\lambda'}^{nr*} + a_{0\lambda}^{nr} b_0^{\rho*}] \\ &= 2[a_{+}^{\rho} a_{+\lambda'}^{nr} \cos(\delta_{+}^{\rho} - \delta_{+\lambda'}^{nr}) - a_{-}^{\rho} a_{-\lambda'}^{nr} \cos(\delta_{-}^{\rho} - \delta_{-\lambda'}^{nr})], \quad (50) \end{aligned}$$

$$\begin{aligned} \mathcal{E} &= 4(\sin \gamma) \text{Re} [a_{0\lambda}^{\rho} b_{0\lambda}^{nr*} - a_{0\lambda}^{nr} b_0^{\rho*}] \\ &= -2[a_{+}^{\rho} a_{+\lambda}^{nr} \sin(\delta_{+}^{\rho} - \delta_{+\lambda}^{nr}) - a_{-}^{\rho} a_{-\lambda}^{nr} \sin(\delta_{-}^{\rho} - \delta_{-\lambda}^{nr})], \quad (51) \end{aligned}$$

$$\begin{aligned} \mathcal{E}' &= 4(\sin \gamma) \text{Im} [-a_{0\lambda}^{\rho} b_{0\lambda}^{nr*} + a_{0\lambda}^{nr} b_0^{\rho*}] \\ &= 2[a_{+}^{\rho} a_{+\lambda}^{nr} \sin(\delta_{+}^{\rho} - \delta_{+\lambda}^{nr}) + a_{-}^{\rho} a_{-\lambda}^{nr} \sin(\delta_{-}^{\rho} - \delta_{-\lambda}^{nr})], \quad (52) \end{aligned}$$

$$\begin{aligned} \mathcal{F} &= 4(\sin \gamma) \text{Im} [a_0^f b_0^{\rho*} + a_0^{\rho} b_0^{f*}] \\ &= 2[a_{+}^{\rho} a_{+}^f \cos(\delta_{+}^{\rho} - \delta_{+}^f) - a_{-}^{\rho} a_{-}^f \cos(\delta_{-}^{\rho} - \delta_{-}^f)], \quad (53) \end{aligned}$$

$$\begin{aligned}\mathcal{G} &= 4(\sin \gamma) \text{Re} \left[a_0^f b_0^{\rho*} - a_0^{\rho} b_0^{f*} \right] \\ &= 2[a_+^{\rho} a_+^f \sin(\delta_+^{\rho} - \delta_+^f) - a_-^{\rho} a_-^f \sin(\delta_-^{\rho} - \delta_-^f)],\end{aligned}\quad (54)$$

$$\begin{aligned}\mathcal{H} &= 4(\sin \gamma) \text{Im} \left[a_0^f b_{0\lambda}^{nr*} + a_{0\lambda}^{nr} b_0^{f*} \right] \\ &= 2[a_+^f a_{+\lambda}^{nr} \cos(\delta_+^f - \delta_{+\lambda}^{nr}) - a_-^f a_{-\lambda}^{nr} \cos(\delta_-^f - \delta_{-\lambda}^{nr})],\end{aligned}\quad (55)$$

$$\begin{aligned}\mathcal{H}' &= 4(\sin \gamma) \text{Im} \left[a_0^f b_{0\lambda'}^{nr*} + a_{0\lambda'}^{nr} b_0^{f*} \right] \\ &= 2[a_+^f a_{+\lambda'}^{nr} \cos(\delta_+^f - \delta_{+\lambda'}^{nr}) - a_-^f a_{-\lambda'}^{nr} \cos(\delta_-^f - \delta_{-\lambda'}^{nr})],\end{aligned}\quad (56)$$

$$\begin{aligned}\mathcal{P} &= 4(\sin \gamma) \text{Re} \left[a_0^f b_{0\lambda}^{nr*} - a_{0\lambda}^{nr} b_0^{f*} \right] \\ &= -2[a_+^f a_{+\lambda}^{nr} \sin(\delta_+^f - \delta_{+\lambda}^{nr}) - a_-^f a_{-\lambda}^{nr} \sin(\delta_-^f - \delta_{-\lambda}^{nr})],\end{aligned}\quad (57)$$

$$\begin{aligned}\mathcal{P}' &= 4(\sin \gamma) \text{Im} \left[-a_0^f b_{0\lambda'}^{nr*} + a_{0\lambda'}^{nr} b_0^{f*} \right] \\ &= 2[a_+^f a_{+\lambda'}^{nr} \sin(\delta_+^f - \delta_{+\lambda'}^{nr}) + a_-^f a_{-\lambda'}^{nr} \sin(\delta_-^f - \delta_{-\lambda'}^{nr})],\end{aligned}\quad (58)$$

and

$$\mathcal{Q} = 4(\sin \gamma) \text{Im} \left[a_0^f b_0^{f*} \right] = (a_+^f)^2 - (a_-^f)^2. \quad (59)$$

In the previous work of Ref. [2], we used a different form for the $KK \rightarrow \pi\pi$ amplitude, writing it as $|K_\lambda| \cos(\delta_\lambda + \delta_{\lambda'} + \Phi_\lambda)$, where $K_\lambda = B_{0\lambda}^* A_{0\lambda'} - B_{0\lambda} A_{0\lambda'}^*$ and $\Phi_\lambda = -i \ln(K_\lambda/|K_\lambda|)$. This form is analogous of that used in Eq. (44), in terms of \mathcal{B} and \mathcal{B}' . The phase Φ_λ was chosen to be zero that is the same as to take $\mathcal{B}' = 0$, assumed hereafter.

As a remark, we call the reader attention that for the compound contribution, we have discarded three-body rescattering effects at the two-loop level since they are small compared to the first two-body collision contribution, as suggested by the three-body model calculations for the $D^\pm \rightarrow K^\pm \pi^+ \pi^-$ decay, see Refs. [28–30].

VI. ANALYSIS OF CP ASYMMETRY TERMS

In order to be able to compare our model directly with the recent experimental data regarding the $B^\pm \rightarrow \pi^\pm \pi^+ \pi^-$ and $B^\pm \rightarrow K^\pm \pi^+ \pi^-$ decays presented in Ref. [9], we had to eliminate one variable in Eq. (44), namely, the square mass of the pair presenting the bachelor particle. We perform this calculation in Appendix A. Here in this section, we show the behavior of some terms of the integrated Eq. (44).

A. Direct CPV term containing the \mathcal{C} parameter

As it was mentioned before, the term of the integrated Eq. (44) containing the \mathcal{C} parameter, is equivalent to the direct CPV induced by the interference between the tree and penguin amplitudes with one meson resonance in

the final state. In this case, the contribution from CPV comes only from the $\rho(770)$ meson. In Fig. 2, we show the signature of the CPV from this term with the usual Breit-Wigner square modulus and with the same sign for both cases, namely, $\cos \theta < 0$ and $\cos \theta > 0$. This term locally violates the CPT constraint and will be set to zero in our fittings, by assuming $\mathcal{C} = 0$.

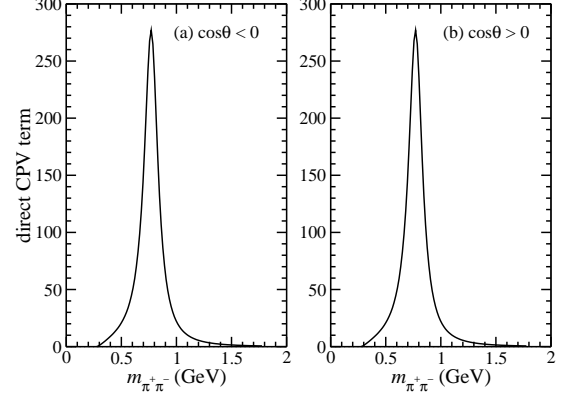


FIG. 2. Term containing the \mathcal{C} parameter of the integrated Eq. (44), as a function of $m_{\pi^+\pi^-} = \sqrt{s}$ for (a) $\cos \theta < 0$ and (b) $\cos \theta > 0$. In these plots we set $\mathcal{C} = 1$.

B. DCPV term containing the \mathcal{D} parameter

The Dalitz CPV induced by the interference term of the integrated Eq. (44), namely, that containing the \mathcal{D} parameter, is directly related with the real part of the Breit-Wigner function. This function presents a clear signature in the mass spectrum, namely, a zero and a change in the sign of the CP asymmetry at the central value of the $\rho(770)$ mass. Another peculiarity associated to vector mesons resonances is one more sign change when the $\cos \theta$ cross the zero around the middle of the Dalitz plot. These two facts can be observed in Fig. 3. Notice that this term sums to zero and thus locally satisfies the CPT constraint.

C. DCPV term containing the \mathcal{E} parameter

The term containing the \mathcal{E} parameter in the integrated Eq. (44), associated to the Dalitz CPV induced by the interference between the $\rho(770)$ and the non resonant amplitude, is directly related with the imaginary part of the Breit-Wigner function of $\rho(770)$. The shape is similar to the those presented in Fig. 2, with the clear difference that the proportionality with $\cos \theta$ changes the sign of the CP asymmetry when $\cos \theta$ pass through zero in the middle of the Dalitz plot. Fig. 4 shows these features. Notice that this term sums to zero and thus locally satisfies the CPT constraint.

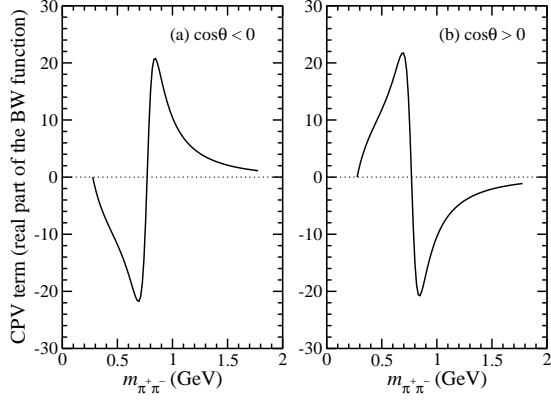


FIG. 3. Term containing the \mathcal{D} parameter of the integrated Eq. (44), as a function of $m_{\pi^+\pi^-} = \sqrt{s}$ for (a) $\cos\theta < 0$ and (b) $\cos\theta > 0$. Here we have used $\Lambda_\lambda = 1.705$ GeV and $\mathcal{D} = 1$.

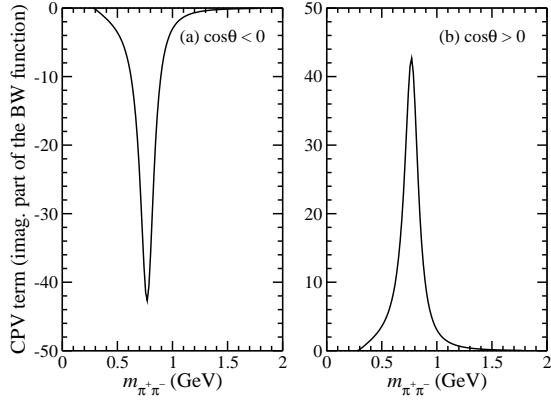


FIG. 4. Term containing the \mathcal{E} parameter of the integrated Eq. (44), as a function of $m_{\pi^+\pi^-} = \sqrt{s}$ for (a) $\cos\theta < 0$ and (b) $\cos\theta > 0$. Here we have used $\Lambda_\lambda = 1.705$ GeV and $\mathcal{E} = 1$.

D. DCPV term containing the \mathcal{F} parameter

The projection of the difference between B^- and B^+ events presents a clear signature in the mass spectrum with a zero close to the mass of the vector meson ρ , and another one close to the mass of the scalar $f_0(980)$. There is also a change of sign in the CP asymmetry associated to the $\cos\theta$ passing through zero around the middle of the Dalitz plot. These features can be observed in Fig. 5, where we display the term containing the \mathcal{F} parameter of the integrated Eq. (44). This term locally satisfies the CPT constraint.

E. DCPV term containing the \mathcal{G} parameter

The shape of this term presents the characteristic peaks of the two interfering resonances. Due to the direct proportionality to $\cos\theta$, there is a change of sign of the CP asymmetry when $\cos\theta$ pass through zero in the middle of the Dalitz plot. Fig. 6 shows the features of this

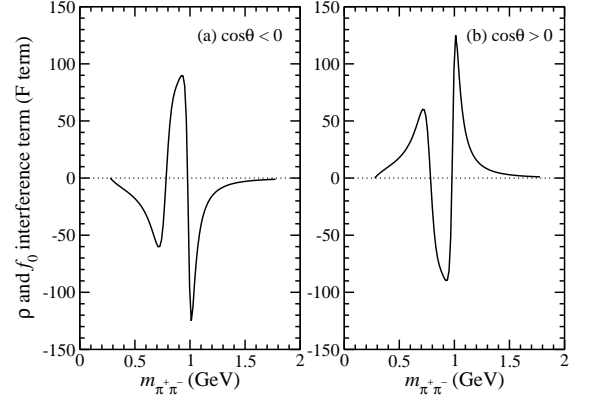


FIG. 5. Term containing the \mathcal{F} parameter of the integrated Eq. (44), as a function of $m_{\pi^+\pi^-} = \sqrt{s}$ for (a) $\cos\theta < 0$ and (b) $\cos\theta > 0$. Here we set $\mathcal{F} = 1$.

term. This term is consistent with the CPT constraint locally.

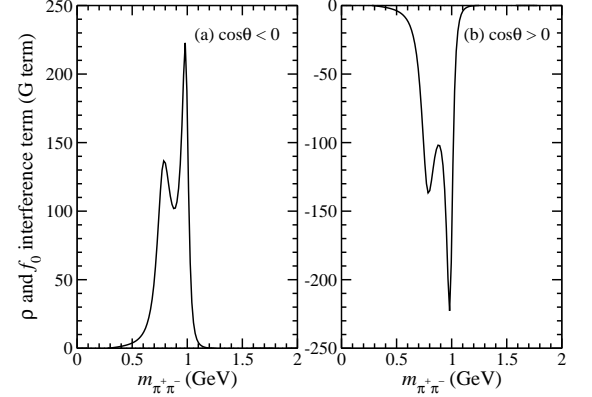


FIG. 6. Term containing the \mathcal{G} parameter of the integrated Eq. (44), as a function of $m_{\pi^+\pi^-} = \sqrt{s}$ for (a) $\cos\theta < 0$ and (b) $\cos\theta > 0$. Here we set $\mathcal{G} = 1$.

VII. CPV IN $B^\pm \rightarrow \pi^\pm \pi^+ \pi^-$ AND $B^\pm \rightarrow \pi^\pm K^+ K^-$ DECAYS

We determine the relative contributions related to the integrated Eq. (44) by fitting two CP asymmetries distributions presented in Ref. [9]; one for the $\pi^+\pi^-$ mass distribution coming from the difference between B^- and B^+ in $B^\pm \rightarrow \pi^\pm \pi^+ \pi^-$ decay, in particular the distribution with $\cos\theta > 0$. From this fitting we found the parameters and plot the CP asymmetry for $\cos\theta < 0$. The other fit was performed for the phase-space integration in the region $\cos\theta < 0$ of the $\pi^+\pi^-$ mass distributions in the $B^\pm \rightarrow K^\pm \pi^+ \pi^-$ decay. From these two fits we get the value of the $\pi^+\pi^- \rightarrow K^+ K^-$ parameter (\mathcal{B}) for each decay channel and plot the asymmetry for the $K^+ K^-$ distribution in the channels $B^\pm \rightarrow \pi^\pm K^+ K^-$ and $B^\pm \rightarrow K^\pm K^+ K^-$.

To perform both fits and the other plots, we use the $\pi^+\pi^- \rightarrow K^+K^-$ amplitude, the non resonant component, and the ρ and $f_0(980)$ resonances. We put these amplitudes within the isobar model through a coherent sum of them. The biggest source of uncertainty from these fits is the error in the $\pi\pi$ phase shift and inelasticity parameter. For simplicity we use the central value of Ref. [26], although possible variations within the quoted errors in the parameters could give better results. Despite our belief that this model is able to represent much of this data, we are aware that it can not explain all the rich CP violation structure observed in these decays. The inclusion of other contributions and the symmetrization of the $B^\pm \rightarrow \pi^\pm\pi^+\pi^-$ decay amplitude would be necessary to understand in more details the phase space of these decays and get better agreement in all CP asymmetry regions presented in Ref. [9].

To perform the fits we use for the $f_0(980)$ resonance, $m_f = 0.975$ GeV and width $\Gamma'_f = 0.044$ GeV, getting from E791 experiment [27]. For the two Λ parameters, we use $\Lambda_\lambda = \Lambda_{\pi\pi} = 3.0$ GeV and $\Lambda_{\lambda'} = \Lambda_{KK} = 4.0$ GeV. It is important to say that we changed these values by a factor two without finding an appreciable change in the fitting.

A. $\pi\pi\pi$ channel

We started by performing the fit of the integrated Eq. (44) to the $\cos\theta > 0$ asymmetry distribution of the low $\pi^+\pi^-$ mass projection for the $B^\pm \rightarrow \pi^\pm\pi^+\pi^-$ decay. Due the presence of identical particles in final state, the interference between symmetrical terms by the exchange of the two identical pions must disturb the CP violation pattern mostly for $\cos\theta < 0$. We study the regions on the Dalitz plot where this interference can be minimum and observe that it corresponds to the high $\pi^+\pi^-$ region on the $\cos\theta > 0$ distribution as can be seen in Fig. 7.

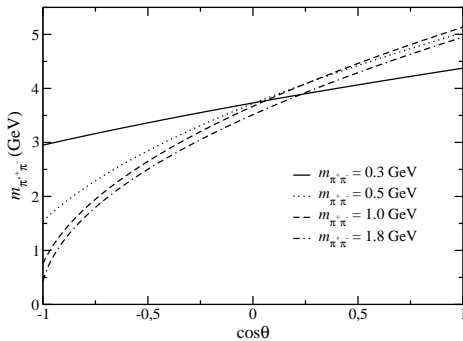


FIG. 7. $m_{\pi^+\pi^-}$ as a function of $\cos\theta$ for some particular values of $m_{\pi^+\pi^-}$.

This figure provides the mass of the changeless pair of pions formed with the bachelor pion. If $\cos\theta < 0$ the mass of this pair stays below 3 GeV, and for $m_{\pi^+\pi^-} \lesssim 1$ GeV, it can be even below 1 GeV, and therefore mak-

ing relevant the interference with the resonances. For $\cos\theta > 0$, $m_{\pi^+\pi^-} > 3$ GeV, minimizing interference effects from the Bose symmetrization of the decay amplitude. We intend to perform this study in the future. For the moment, we do not consider the symmetrization of the decay amplitude, and therefore we do not use the data for the CP asymmetry in the $B^\pm \rightarrow \pi^\pm\pi^+\pi^-$ channel for $\cos\theta < 0$ to fit the parameters.

The best fit was obtained by using four parameters associated to the $\pi^+\pi^- \rightarrow K^+K^-$ amplitude (\mathcal{B}), the real and imaginary parts of the interference between the ρ and the non resonant partonic amplitudes (\mathcal{D} and \mathcal{E}), and finally the imaginary part of the interference between the ρ and the $f_0(980)$ resonances (\mathcal{G}). The result is presented in Fig. 8a, where we compared our model with the experimental data extracted from Fig. 4c of Ref. [9]. The remaining parameters, namely, those that locally violate the CPT constraint, and those negligible in the fitting procedure, were set to zero.

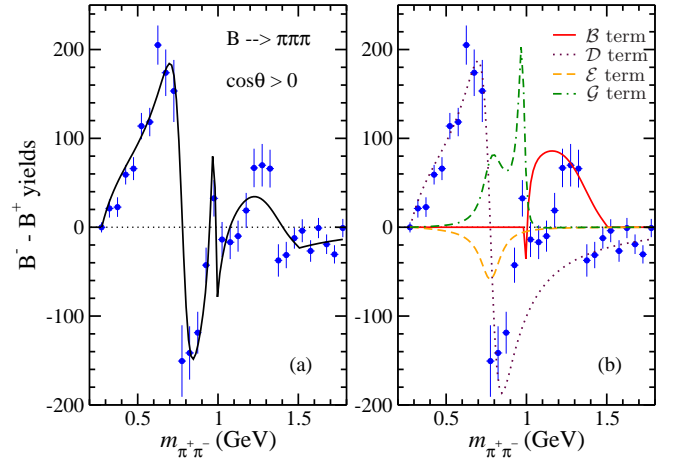


FIG. 8. (Color online) CP asymmetry of the $B^\pm \rightarrow \pi^\pm\pi^+\pi^-$ decay, integrated Eq. (44), compared with the experimental values (blue points) taken from Ref. [9]. Results for $\cos\theta > 0$ for (a) total and (b) individual contributions.

The individual contributions to the CP asymmetry are shown in Fig. 8b. As expected, the ρ meson contribution represented by the amplitudes containing the \mathcal{D} and \mathcal{E} parameters, is large mainly for the real part of the BW, and the presence of $f_0(980)$ is seen only by one of the interfering terms with the ρ , namely, that presenting the \mathcal{G} parameter. All these terms are locally CPT invariant, namely by integration in $\cos\theta$ their contribution to the CP asymmetry vanishes. Between 1 and 1.6 GeV, the contribution of the $\pi^+\pi^- \rightarrow K^+K^-$ amplitude, namely, the \mathcal{B} term, shows its importance and as expected [2], dominates the asymmetry in this region. We remind that this part of the asymmetry does not vanishes upon integration in $\cos\theta$ and cancels the asymmetry in the $B^\pm \rightarrow \pi^\pm K^+K^-$ decay channel.

Looking at the behavior of the experimental $\cos\theta < 0$ distribution in Fig. 9a, we can see that much of the fea-

tures observed for the distribution of events for $\cos\theta > 0$ are present in this asymmetry. In fact, we plotted together with the experimental points, the amplitudes computed with the integrated Eq. (44) using the fit parameters obtained from the $\cos\theta > 0$ distribution. The plot in Fig. 9a shows a clear departure from the experimental data when at the starting of the ρ mass resonance and also at the beginning of the contribution of the $\pi^+\pi^- \rightarrow K^+K^-$ amplitude to the asymmetry. Assuming that these differences are due to the symmetrization, this result suggests an interference between ρ and $\pi^+\pi^- \rightarrow K^+K^-$ amplitude in the crossing channels, which is corroborated by Fig. 7, where for the mass region above 1 GeV, the mass of the $\pi^+\pi^-$ pair in the crossing channel for $\cos\theta \lesssim -0.75$ can be even below 1 GeV. In addition, we show in Fig. 9b the individual contributions to this CP asymmetry distribution.

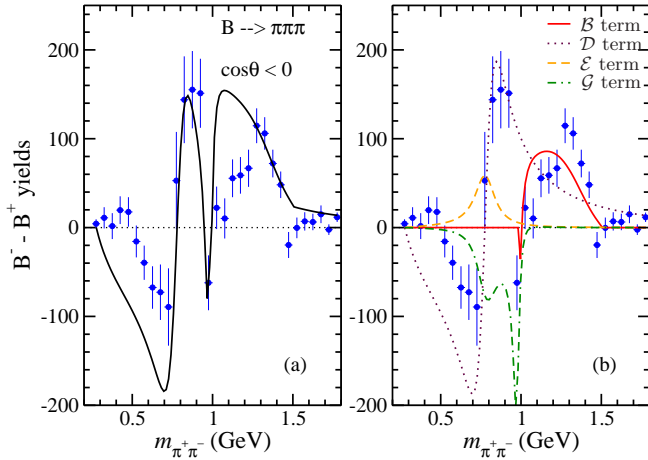


FIG. 9. (Color online) CP asymmetry of the $B^\pm \rightarrow \pi^\pm\pi^+\pi^-$ decay, integrated Eq. (44), compared with the experimental values (blue points) taken from Fig. 4d of Ref. [9]. Results for $\cos\theta < 0$ for (a) total and (b) individual contributions.

We still remark to the reader that for the $B^\pm \rightarrow \pi^\pm\pi^+\pi^-$ decay, our definition of the angle θ is opposite from that presented in Ref. [9]. Thus, we had to compare our results of $\cos\theta > 0$ ($\cos\theta < 0$) with those of $\cos\theta < 0$ ($\cos\theta > 0$) of Ref. [9].

B. πKK channel

The expression for the CP asymmetry in the coupled $B^\pm \rightarrow \pi^\pm K^+K^-$ channel, derived from the general formula in Eq. (29), applied to this specific decay and integrated in $\cos\theta$, is given by

$$\Delta\Gamma(s) = -\frac{2\mathcal{A}}{a'(s)\sqrt{s-4m_K^2}\left(1+\frac{s}{\Lambda_{\lambda'}^2}\right)^2} - \frac{2\mathcal{B}\sqrt{1-\eta^2(s)}\cos[2\delta_{\pi\pi}(s)]}{a'(s)\sqrt{s-4m_K^2}\left(1+\frac{s}{\Lambda_{\lambda'}^2}\right)\left(1+\frac{s}{\Lambda_{\lambda''}^2}\right)}, \quad (60)$$

where the kinematical factors, namely,

$$a'(s) = \frac{1}{(s-4m_K^2)^{1/2} \left[\frac{(M_B^2-m_\pi^2-s)^2}{4s} - m_\pi^2 \right]^{1/2}}, \quad (61)$$

and the kaon momentum in the rest frame of the KK subsystem, $\sqrt{s-4m_K^2}$, are now taken for the πKK system. Furthermore, the integrated decay width in $\cos\theta$ from Eq. (60), becomes exactly opposite in sign to the decay width in the $\pi\pi\pi$ channel above the KK threshold, c.f. the first two terms of the integrated Eq. (44).

The expression in Eq. (60) is obtained by adding the $\pi^+\pi^- \rightarrow K^+K^-$ contributions detailed in Figs. 8 and 9, since $\mathcal{A} = 0$. The plot shown in Fig. 10 was done with the parameters fitted by the CP asymmetry data in the $B^\pm \rightarrow \pi^\pm\pi^+\pi^-$ decay. The CP violation distribution obtained for the K^+K^- invariant mass from $B^\pm \rightarrow \pi^\pm K^+K^-$ decay through Eq. (60), has opposite sign with respect to the correspondent term in the coupled $\pi^\pm\pi^+\pi^-$ channel.

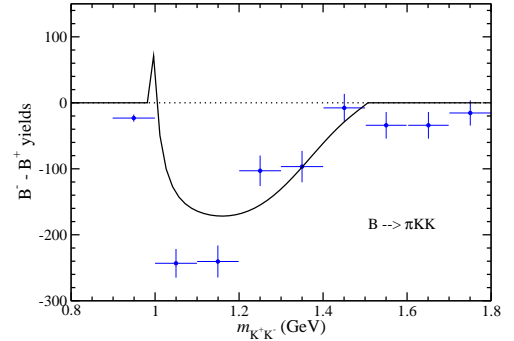


FIG. 10. (Color online) CP asymmetry of the $B^\pm \rightarrow \pi^\pm K^+K^-$ decay, Eq. (60), compared with experimental data (blue points) taken from Fig. 7b of Ref. [9].

For this decay, the LHCb experiment presented the sum of events with $\cos\theta < 0$ and $\cos\theta > 0$. The comparison of the data with our model is also provided in Fig. 10. There is a clear agreement about the shape of the model distribution with the experimental data and also a reasonable amount of the number of events related with this kind of CP asymmetry. It is also worth to mention that CPT is conserved if we sum all CP asymmetry contributions obtained with our approach to $B^\pm \rightarrow \pi^\pm\pi^+\pi^-$ and $B^\pm \rightarrow \pi^\pm K^+K^-$ decays, in a region of $\pi^+\pi^-$ and K^+K^- invariant mass below 1.6 GeV.

VIII. CPV IN $B^\pm \rightarrow K^\pm\pi^+\pi^-$ AND $B^\pm \rightarrow K^\pm K^+K^-$ DECAYS

The number of events observed in these two decay channels are about one order of magnitude larger than in the $\pi^\pm\pi^+\pi^-$ and $\pi^\pm K^+K^-$ data [9]. This allows a better fit to the difference between B^- and B^+ events. In the fitting procedure we use only the $\cos\theta < 0$ distribution, because the experimental results [9] for $\cos\theta > 0$

present a new feature in both decays in the region studied in this work. Our simple model does not account for this new behavior. We only have a guess, that we already mentioned in our previous paper [2], related with the possible presence of re-scattering coming from double charm decays. One should note that three light-pseudoscalar mesons can, in principle, couple via strong interaction with channels like $D\bar{D}K$. It seems reasonable to expect that $D\bar{D}K \rightarrow KKK$ or $K\pi\pi$ can contribute to the CP asymmetry in regions of large two-body invariant mass above the $D\bar{D}$ threshold, that is far from the KK threshold and above 1.6 GeV, outside the region discussed in this work but excluded from the $\cos\theta < 0$ distribution.

A. $K\pi\pi$ channel

Differently to the $B^\pm \rightarrow \pi^\pm\pi^+\pi^-$ decay where the ρ amplitudes were dominant, here the $f_0(980)$ has the largest contribution to the $B^\pm \rightarrow K^\pm\pi^+\pi^-$ decay, as it is expected by recalling the BSS mechanism applied to these decays, which builds in principle the corresponding amplitudes associated with the source terms or partonic amplitudes. One possible good fit for the integrated Eq. (44) is obtained by using five parameters associated to the $\pi^+\pi^- \rightarrow K^+K^-$ amplitude (\mathcal{B}), the real parts of the interference between ρ resonance with the non resonant partonic (\mathcal{D}), and $\pi^+\pi^- \rightarrow K^+K^-$ amplitudes (\mathcal{D}'), and finally the real and imaginary parts of the interference between the ρ and the $f_0(980)$ resonances, (\mathcal{F} and \mathcal{G}). As in the $B^\pm \rightarrow \pi^\pm\pi^+\pi^-$ case, the parameters that locally violate the CPT constraint, and those negligible in the fitting procedure were set to zero. Fig. 11a shown the best fit we get to the $\cos\theta < 0$ distribution.

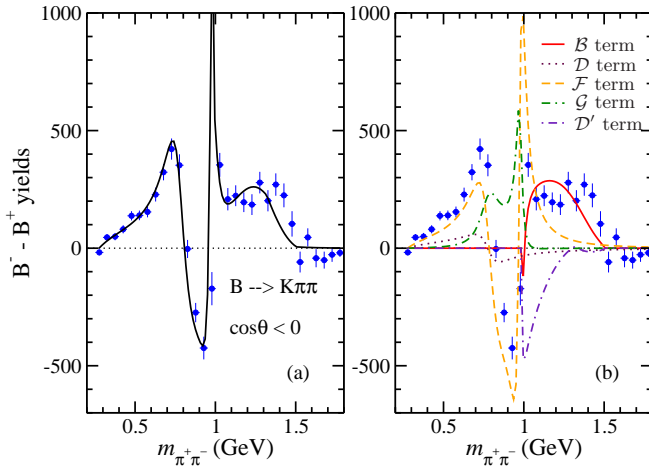


FIG. 11. (Color online) CP asymmetry of the $B^\pm \rightarrow K^\pm\pi^+\pi^-$ decay, integrated Eq. (44), compared with the experimental values (blue points) taken from Fig. 5c of Ref. [9]. Results for $\cos\theta < 0$ for (a) total and (b) individual contributions.

In Fig. 11b, we shown the decomposition of each component of the fit. Clearly the dominant contribution

comes from the real part of the interference between ρ and the $f_0(980)$ resonances. The imaginary part of this amplitude has a contribution, however, much less important than the real one. The $\pi^+\pi^-$ and K^+K^- amplitude plays an important role in this fit above 1 GeV and also associated with the interference with the ρ resonance.

Here, we also used $\Lambda_\lambda = 3.0$ GeV and $\Lambda_{\lambda'} = 4.0$ GeV. The other parameters were found by using the χ^2 method in order to fit the experimental data for $\cos\theta < 0$ distribution from Ref. [9].

B. KKK channel

The CP asymmetry in the B^- and B^+ event distributions in the $B^\pm \rightarrow K^\pm K^+ K^-$ channel is compared to our model with the sum of the events of $\cos\theta < 0$ and $\cos\theta > 0$ as we did for $B^\pm \rightarrow \pi^\pm K^+ K^-$ decay channel and the data provided by the LHCb in this last case. The functional form of the asymmetry for the $B^\pm \rightarrow K^\pm K^+ K^-$ decay is the same as in Eq. (60). The only change is due to the kinematical factor $a'(s)$ in Eq. (61), that now presents the replacement $m_\pi \rightarrow m_K$.

We plot in Fig. 12 the asymmetry of the $B^\pm \rightarrow K^\pm K^+ K^-$ decay, computed with the parameter \mathcal{B} obtained in our previous fitting of the $B^\pm \rightarrow K^\pm\pi^+\pi^-$ decay. Our model is compared to the data obtained by summing the experimental results of $B^\pm \rightarrow K^\pm K^+ K^-$ distributions for both $\cos\theta$ positive and negative regions.

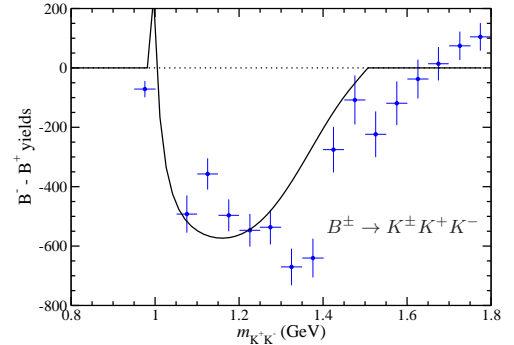


FIG. 12. CP asymmetry of the $B^\pm \rightarrow K^\pm K^+ K^-$ decay compared with experimental values (blue points) taken from the sum of Figs. 6c and 6d of Ref. [9].

IX. CONCLUDING REMARKS

A. Beyond the model

We can go beyond the asymmetry formula in Eq. (38), where we have not included the interference terms between the resonances and the scattering terms in the elastic channel, we remind that in the BW we included the elastic amplitude, but it is also important to consider it

outside the resonance region, and returning to (29) as the starting point. We have neglected the Bose symmetrization of the amplitude by the exchange of the identical pions and the contribution of the double charm production and the its coupling to the KK channel. This also should be addressed in the future.

The isoscalar and zero angular momentum $\pi\pi$ originated by contribution of the elastic scattering terms to the CP asymmetry for $B^\pm \rightarrow \pi^\pm \pi^+ \pi^-$ and $B^\pm \rightarrow K^\pm \pi^+ \pi^-$ decays written before, can be substituted the inelasticity and phase-shifts given by $\pi\pi \rightarrow KK$ S-matrix provided by Eq. (39) as $t_{\pi\pi, \pi\pi}^{J=0} = i(1 - \eta e^{2i\delta_{\pi\pi}})$. The inclusion of the S -wave $\pi\pi$ scattering should improve the fitting below the ρ , where it is clearly seen in Fig. 9, the effect of a missing interference term. In this particular region the $f_0(600)$, namely the σ , will be taken into account by $t_{\pi\pi, \pi\pi}^{J=0}$, and we expect to improve the fit in the low mass region.

The interference between $\pi\pi \rightarrow KK$ and the ρ resonance was used to fit the $K\pi\pi$ channel, as we can see in Fig. 11. Other possibility in this fit would be consider the large presence of $f_0(980)$, by using its interference with $\pi\pi \rightarrow KK$. This component do not satisfy CPT locally, but is consistent with Eq. (29) with the coupled channel $B^\pm \rightarrow K^\pm K^+ K^-$. In this work, we choose to use only locally CPT invariant components for the interference with resonances.

B. Conclusions

We show how CP asymmetry in charmless three-body B^\pm decays is constrained by CPT in the presence of resonances and final state interaction in leading order. The CPT constraint $\sum_\lambda \Delta\Gamma_\lambda = 0$, should include in the sum over the final states, all the kinematical allowed phase space and possible decay channels. In leading order, the scattering matrix $t_{\lambda, \lambda}$ corresponding to the decay channel where a resonance is formed, e.g., the ρ in p-wave $\pi\pi$ elastic amplitude, accounts for the dressing of the decay vertex $\rho \rightarrow \pi\pi$. The physical decay amplitudes associated with the partonic source, that give the ρ meson and in its sequential decay to two pions, is dressed by the $\pi\pi$ re-scattering process in the resonant channel. The non-resonant channels receive contribution from the re-scattering in leading order. The decay of the resonance and re-scattering by the bachelor meson, should appear as a next-to-leading order contribution, to be consider in future works, where the general formulas for the three-body decay amplitude based on the CPT constraint that includes the formation of resonances, re-scattering and coupling to inelastic channels should be addressed. In our limited two-body description, we explored the rich patterns of the CP asymmetry formula, namely interference between non-resonant and resonant terms, as well as the coupling between the $\pi\pi$ and KK channels due to the strong interaction.

We analysed in our study two examples of CP viola-

tion in charmless B^\pm three-body decays in the presence of resonances, excluding the possibility of channel coupling. The first case discussed is the $\rho(770)$ meson resonance plus a non resonant channel, and the second one is the case of two interfering resonances, namely, $\rho(770)$ and $f_0(980)$. These examples discussed within two amplitude models are suitable for the study of $B^\pm \rightarrow \pi^\pm \pi^+ \pi^-$ and $B^\pm \rightarrow K^\pm \pi^+ \pi^-$ for $\pi^\pm \pi^\mp$ masses below the KK threshold, as provided by the new data LHCb data [9], and we selected terms that are locally constrained by CPT.

The CP asymmetry produced by the $\rho(770)$ meson resonance in the simple two amplitude model with a non-resonant channel, which are brought by the real and imaginary parts of the interference term, presents a clear signature in the low mass $\pi^+ \pi^+$ spectrum for both decays $B^\pm \rightarrow \pi^\pm \pi^+ \pi^-$ and $B^\pm \rightarrow K^\pm \pi^+ \pi^-$, as indeed the new data suggests [9]. One term shows a very clear signature: a zero at the $\rho(770)$ mass in both regions of $\cos\theta < 0$ and $\cos\theta > 0$ for $B^\pm \rightarrow \pi^\pm \pi^+ \pi^-$ with a change of the sign around $\cos\theta = 0$.

The two amplitude model constituted by the resonances $\rho(770)$ and $f_0(980)$, shows two zeros in the CP asymmetry from the real part of the Breit-Wigners: one close to the $\rho(770)$ mass and another one close to the $f_0(980)$ mass. However, the term which mixes the real and imaginary parts of the Breit-Wigners does not present a clear signature of CP violation around the $\rho(770)$ meson mass, while a zero is present at the $f_0(980)$ mass, because the ratio $\Gamma_\rho m_\rho / \Gamma_f m_f$ is considerably larger than one. In both examples, the zero's of the asymmetry at the resonance mass are associated only with the Dalitz CP violation from the interference of two amplitudes and the real part of the Breit-Wigner, the contributions associated with the imaginary part present a behavior with a maximum at the resonances masses. The recent experimental results [9] are strongly indicating that the CP asymmetry appearing in the low $\pi^+ \pi^+$ mass region comes from the real part of the Breit-Wigners in the interference between two amplitudes involving the ρ meson resonance.

In addition, the CP asymmetries in whole kinematical region below $m_{\pi^+ \pi^-} \lesssim 1.8$ GeV in $B^\pm \rightarrow \pi^\pm \pi^+ \pi^-$ and $B^\pm \rightarrow K^\pm \pi^+ \pi^-$ decays demand the coupling to the $\pi^\pm \pi^+ \pi^-$ by the strong interaction, as has already been discussed in Ref. [2]. To account for that, we introduced in the fitting of the CPV, the contribution of the coupled $\pi\pi$ to KK channels in isoscalar and zero angular states. This was relevant for the fitting above the KK threshold. The independent confirmation of the CP asymmetry flowing between different channels coupled by the strong interaction was checked by the fair reproduction of the CPV in $B^\pm \rightarrow \pi^\pm K^+ K^-$ and $B^\pm \rightarrow K^\pm K^+ K^-$ distributions. The computation of the asymmetry was performed as dictated by the CPT constraint applied to coupled channels. There was no new parameters beyond those given in the fitting of the CP asymmetry data in the $B^\pm \rightarrow \pi^\pm \pi^+ \pi^-$ and $B^\pm \rightarrow K^\pm \pi^+ \pi^-$ decays.

We discussed improvements to CP asymmetry formula

beyond the one used to fit the experimental data on $B^\pm \rightarrow \pi^\pm \pi^+ \pi^-$ decay, where the interference between the resonances and elastic scattering terms are missing. The inclusion of the interference between the S -wave $\pi\pi$ scattering amplitude and the $\rho(770)$ meson Breit-Wigner should improve the fit below the m_ρ . In this particular region, the $f_0(600)$, namely the σ , will be taken into account through the elastic $\pi\pi$ scattering, which it is expected to improve the fit. Still the Bose symmetrization of the amplitude by the exchange of the identical pions has to be considered, which should be addressed in the future.

Finally, the results of our fittings suggest an important consequence to CP violation: the strong phases can come from the hadronic interaction minimizing the effect of the imaginary part of penguin contributions to both decays studied here, as the recent experimental results are indicating.

Appendix A: Angle integrated asymmetry

By defining in Fig. 1, $\pi^+ \equiv 1$, $\pi^- \equiv 2$, and $\pi'^+ \equiv 3$ (bachelor), one has that $m_{\pi^+\pi^-} = m_{12} = \sqrt{s}$, and $m_{\pi'^+\pi^-} = m_{32}$. The kinematics of the decay imposes that $\cos\theta$ is a function of s and m_{32} , namely,

$$\cos\theta = a(s)m_{32}^2 + b(s), \quad (\text{A1})$$

where,

$$a(s) = \frac{1}{(s - 4m_\pi^2)^{1/2} \left[\frac{(M_B^2 - m_\pi^2 - s)^2}{4s} - m_\pi^2 \right]^{1/2}}, \quad (\text{A2})$$

The integration in Eqs. (A4) and (A5) generates the following asymmetry,

$$\begin{aligned} \Delta\Gamma(s) = & \frac{\mathcal{A}}{a(s)\sqrt{s - 4m_\pi^2} \left(1 + \frac{s}{\Lambda_\lambda^2}\right)^2} + \frac{\mathcal{B} \cos[2\delta_{\pi\pi}(s)] \sqrt{1 - \eta^2(s)}}{a(s)\sqrt{s - 4m_\pi^2} \left(1 + \frac{s}{\Lambda_\lambda^2}\right) \left(1 + \frac{s}{\Lambda_{\lambda'}^2}\right)} + \frac{\mathcal{C}|F_\rho^{\text{BW}}(s)|^2 k^2(s)}{3a(s)} \\ & + \frac{|F_\rho^{\text{BW}}(s)|^2 k(s)}{2\xi a(s)} \left\{ \frac{\mathcal{D}(m_\rho^2 - s)}{1 + \frac{s}{\Lambda_\lambda^2}} + \frac{\mathcal{D}' \sqrt{1 - \eta^2(s)} \{m_\rho \Gamma_\rho(s) \cos[2\delta_{\pi\pi}(s)] - (m_\rho^2 - s) \sin[2\delta_{\pi\pi}(s)]\}}{\sqrt{s - 4m_\pi^2} \left(1 + \frac{s}{\Lambda_{\lambda'}^2}\right)} \right\} \\ & + \frac{\mathcal{E} m_\rho \Gamma_\rho(s)}{1 + \frac{s}{\Lambda_\lambda^2}} + \frac{\mathcal{E}' \sqrt{1 - \eta^2(s)} \{ (m_\rho^2 - s) \cos[2\delta_{\pi\pi}(s)] + m_\rho \Gamma_\rho(s) \sin[2\delta_{\pi\pi}(s)] \}}{\sqrt{s - 4m_\pi^2} \left(1 + \frac{s}{\Lambda_{\lambda'}^2}\right)} \Bigg\} \\ & + \frac{|F_\rho^{\text{BW}}(s)|^2 |F_f^{\text{BW}}(s)|^2 k(s)}{2\xi a(s)} \times \\ & \times \{ \mathcal{F}[(m_\rho^2 - s)(m_f^2 - s) + m_\rho \Gamma_\rho(s) m_f \Gamma_f(s)] + \mathcal{G}[(m_\rho^2 - s) m_f \Gamma_f(s) - m_\rho \Gamma_\rho(s) (m_f^2 - s)] \} \\ & + \frac{|F_f^{\text{BW}}(s)|^2}{a(s)} \left\{ \frac{\mathcal{H}(m_f^2 - s)}{1 + \frac{s}{\Lambda_\lambda^2}} + \frac{\mathcal{H}' \sqrt{1 - \eta^2(s)} \{ m_f \Gamma_f(s) \cos[2\delta_{\pi\pi}(s)] - (m_f^2 - s) \sin[2\delta_{\pi\pi}(s)] \}}{\sqrt{s - 4m_\pi^2} \left(1 + \frac{s}{\Lambda_{\lambda'}^2}\right)} \right\} \\ & + \frac{\mathcal{P} m_f \Gamma_f(s)}{1 + \frac{s}{\Lambda_\lambda^2}} + \frac{\mathcal{P}' \sqrt{1 - \eta^2(s)} \{ (m_f^2 - s) \cos[2\delta_{\pi\pi}(s)] + m_f \Gamma_f(s) \sin[2\delta_{\pi\pi}(s)] \}}{\sqrt{s - 4m_\pi^2} \left(1 + \frac{s}{\Lambda_{\lambda'}^2}\right)} \Bigg\} + \frac{\mathcal{Q}|F_f^{\text{BW}}(s)|^2}{a(s)}, \quad (\text{A7}) \end{aligned}$$

and

$$b(s) = - \frac{M_B^2 + 3m_\pi^2 - s}{2(s - 4m_\pi^2)^{1/2} \left[\frac{(M_B^2 - m_\pi^2 - s)^2}{4s} - m_\pi^2 \right]^{1/2}}, \quad (\text{A3})$$

with $M_B = 5.279$ GeV (the detailed derivation of this equation is relegated to the Appendix B). Therefore, the asymmetry presented in Eq. (44) is actually a function of s and m_{32} , due to $\cos\theta$. In order to eliminate m_{32}^2 , we integrate $\Delta\Gamma_\lambda(s, m_{32}^2)$ in this variable, leading to the asymmetry $\Delta\Gamma(s) \equiv \int \Delta\Gamma_\lambda(s, m_{32}^2) dm_{32}^2$. We still separate the integration in two regions, namely, that of $\cos\theta < 0$, leading to

$$\Delta\Gamma(s)^{(\cos\theta < 0)} = \int_{(m_{32}^2)_{-1}}^{-b/a} \Delta\Gamma_\lambda(s, m_{32}^2) dm_{32}^2, \quad (\text{A4})$$

and that of $\cos\theta > 0$, leading to

$$\Delta\Gamma(s)^{(\cos\theta > 0)} = \int_{-b/a}^{(m_{32}^2)_{+1}} \Delta\Gamma_\lambda(s, m_{32}^2) dm_{32}^2. \quad (\text{A5})$$

The quantities

$$(m_{23}^2)_{-1}(s) = -\frac{1 + b(s)}{a(s)}, \quad (m_{23}^2)_{+1}(s) = \frac{1 - b(s)}{a(s)} \quad (\text{A6})$$

correspond, respectively, to $\cos\theta = -1$ and $\cos\theta = +1$, according to Eq. (A1). The quantity $-b/a$ is related to $\cos\theta = 0$.

where $\xi = -1$ for $\cos\theta < 0$, and $\xi = 1$ for $\cos\theta > 0$. Here, the rest frame momentum of the pion, namely, $(s - 4m_\pi^2)^{-1/2}$, is included in the terms presenting interference with the $\pi\pi \rightarrow KK$ amplitude, in order to introduce the kinematical factor in the scattering amplitude. Furthermore, this factor is consistent with the CPT constraint, which indicates that the decay widths for the coupled $\pi\pi\pi$ and πKK channels above the KK threshold is such that $\Delta\Gamma_{\pi\pi\pi} = -\Delta\Gamma_{\pi KK}$, as discussed at the end of Sec. VII B. Finally, we also remind that all free parameters are compatible with the energy quantities of the model, that are in GeV units.

Appendix B: Derivation of Eq. (A1)

In a general way, one has that

$$\begin{aligned} P^\mu P'_\mu &= p^0 p'_0 + p^1 p'_1 + p^2 p'_2 + p^3 p'_3 \\ &= EE' - p_x p'_x - p_y p'_y - p_z p'_z \\ &= EE' - \vec{p} \cdot \vec{p}' = p_0 p'_0 - \vec{p} \cdot \vec{p}'. \end{aligned} \quad (\text{B1})$$

If $P^\mu = P'_\mu$, then Eq. (B1) becomes

$$P^\mu P_\mu = E^2 - \vec{p}^2 = m^2 + \vec{p}^2 - \vec{p}^2 = m^2. \quad (\text{B2})$$

In the $B^+ \rightarrow \pi^+ \pi^+ \pi^-$ decay of Fig. 1, we define $\pi^+ \equiv 1$, $\pi^- \equiv 2$, and $\pi'^+ \equiv 3$ (bachelor). Therefore, $m_{\pi^+ \pi^-} = m_{12} = \sqrt{s}$, $m_{\pi'^+ \pi^-} = m_{32}$, and $m_1 = m_2 = m_3 = m_\pi$, since we have degenerated the pion mass. If we assume that

$$P_{32}^\mu \equiv P_3^\mu + P_2^\mu, \quad (\text{B3})$$

then, these definitions lead to

$$\begin{aligned} m_{32}^2 &= P_{32}^\mu P_{32\mu} = (P_3^\mu + P_2^\mu)(P_{3\mu} + P_{2\mu}) \\ &= P_3^\mu P_{3\mu} + P_3^\mu P_{2\mu} + P_2^\mu P_{3\mu} + P_2^\mu P_{2\mu} \\ &= m_3^2 + p_3^0 p_2^0 - \vec{p}_3 \cdot \vec{p}_2 + p_2^0 p_3^0 - \vec{p}_2 \cdot \vec{p}_3 + m_2^2 \\ &= 2m_\pi^2 + 2p_3^0 p_2^0 - 2\vec{p}_3 \cdot \vec{p}_2 \\ &= 2m_\pi^2 + 2p_3^0 p_2^0 + 2|\vec{p}_3||\vec{p}_2|\cos\theta. \end{aligned} \quad (\text{B4})$$

Thus, $\cos\theta$ is written as

$$\cos\theta = \frac{m_{32}^2 - 2m_\pi^2 - 2p_3^0 p_2^0}{2|\vec{p}_3||\vec{p}_2|}. \quad (\text{B5})$$

In order to write $\cos\theta$ in terms of m_{32}^2 and $m_{12}^2 = s$, it is necessary to find p_2^0 , $|\vec{p}_2|$, p_3^0 , and $|\vec{p}_3|$. The first two quantities can be extracted as follows. Notice that,

$$\begin{aligned} m_{12}^2 &= s = P_{12}^\mu P_{12\mu} = (P_1^\mu + P_2^\mu)(P_{1\mu} + P_{2\mu}) \\ &= P_1^\mu P_{1\mu} + P_1^\mu P_{2\mu} + P_2^\mu P_{1\mu} + P_2^\mu P_{2\mu} \\ &= m_1^2 + p_1^0 p_2^0 - \vec{p}_1 \cdot \vec{p}_2 + p_2^0 p_1^0 - \vec{p}_2 \cdot \vec{p}_1 + m_2^2 \\ &= 2m_\pi^2 + 2p_1^0 p_2^0 - 2\vec{p}_1 \cdot \vec{p}_2 \\ &= 2m_\pi^2 + 2p_1^0 p_2^0 + 2|\vec{p}_1||\vec{p}_2|. \end{aligned} \quad (\text{B6})$$

Furthermore, by the figure, we see that $|\vec{p}_1| = |\vec{p}_2| \equiv |\vec{p}_\pi|$. However, since $p_1^0 = \sqrt{m_\pi^2 + |\vec{p}_1|^2}$ and $p_2^0 = \sqrt{m_\pi^2 + |\vec{p}_2|^2}$, we conclude that $p_1^0 = p_2^0 \equiv p_\pi^0 = \sqrt{m_\pi^2 + |\vec{p}_\pi|^2}$. Then,

$$s = 2m_\pi^2 + 2(m_\pi^2 + |\vec{p}_\pi|^2) + 2|\vec{p}_\pi|^2 = 4m_\pi^2 + 4|\vec{p}_\pi|^2, \quad (\text{B7})$$

with

$$|\vec{p}_\pi| = \sqrt{\frac{s}{4} - m_\pi^2}, \quad (\text{B8})$$

and

$$p_\pi^0 = \sqrt{m_\pi^2 + |\vec{p}_\pi|^2} = \frac{\sqrt{s}}{2}. \quad (\text{B9})$$

In order to find the s dependence of p_3^0 and $|\vec{p}_3|$, we proceed to write

$$P_B^\mu = P_1^\mu + P_2^\mu + P_3^\mu = P_{12}^\mu + P_3^\mu, \quad (\text{B10})$$

and make

$$\begin{aligned} M_B^2 &= P_B^\mu P_{B\mu} = (P_{12}^\mu + P_3^\mu)(P_{12\mu} + P_{3\mu}) \\ &= P_{12}^\mu P_{12\mu} + P_{12}^\mu P_{3\mu} + P_3^\mu P_{12\mu} + P_3^\mu P_{3\mu} \\ &= s + p_{12}^0 p_3^0 - \vec{p}_{12} \cdot \vec{p}_3 + p_3^0 p_{12}^0 - \vec{p}_3 \cdot \vec{p}_{12} + m_3^2. \end{aligned} \quad (\text{B11})$$

In the reference frame in which $\vec{p}_{12} = \vec{p}_1 + \vec{p}_2 = 0$, we have

$$M_B^2 = s + 2p_{12}^0 p_3^0 + m_3^2. \quad (\text{B12})$$

Furthermore, in this reference frame, $p_{12}^0 = \sqrt{s + |\vec{p}_{12}|^2} = \sqrt{s}$, leading to

$$M_B^2 = s + 2\sqrt{s}p_3^0 + m_\pi^2. \quad (\text{B13})$$

From this equation we get,

$$p_3^0 = \frac{M_B^2 - m_\pi^2 - s}{2\sqrt{s}}. \quad (\text{B14})$$

Finally, from $p_3^0 = \sqrt{m_\pi^2 + |\vec{p}_3|^2}$, we have

$$\begin{aligned} |\vec{p}_3| &= \sqrt{(p_3^0)^2 - m_\pi^2} \\ &= \sqrt{\frac{(M_B^2 - m_\pi^2 - s)^2}{4s} - m_\pi^2}. \end{aligned} \quad (\text{B15})$$

Inserting Eqs. (B8), (B9), (B14) and (B15) in Eq. (B5) we get,

$$\begin{aligned} \cos\theta &= \frac{m_{32}^2 - 2m_\pi^2 - \frac{M_B^2 - m_\pi^2 - s}{2}}{2\left(\frac{s}{4} - m_\pi^2\right)^{1/2} \left[\frac{(M_B^2 - m_\pi^2 - s)^2}{4s} - m_\pi^2\right]^{1/2}} \\ &= \frac{2m_{32}^2 - M_B^2 - 3m_\pi^2 + s}{2(s - 4m_\pi^2)^{1/2} \left[\frac{(M_B^2 - m_\pi^2 - s)^2}{4s} - m_\pi^2\right]^{1/2}}. \end{aligned} \quad (\text{B16})$$

This same equation is obtained if we now treat the $B^- \rightarrow \pi^- \pi^+ \pi^-$ decay. In this case, the B meson and the pions of Fig. 1 have its charges changed, and one defines $\pi^- \equiv 1$, $\pi^+ \equiv 2$ and $\pi'^- \equiv 3$ (bachelor). Therefore, one has $m_{\pi^+ \pi^-} = m_{21} = \sqrt{s}$, and $m_{\pi^+ \pi'^-} = m_{23}$. For this case, $\cos\theta$ will be written exactly as in Eq. (B16), but for $m_{32} \rightarrow m_{23}$.

ACKNOWLEDGMENTS

We thank the support from Conselho Nacional de Desenvolvimento Científico e Tecnológico (CNPq) of

Brazil. O. L. also acknowledges the support of the grant #2013/26258-4 from São Paulo Research Foundation (FAPESP). J. H. A. N. acknowledges the support of the grant #2014/19094-8 from São Paulo Research Foundation (FAPESP).

-
- [1] I. I. Bigi, *Front. Phys.* **10**, 101203 (2015).
 - [2] I. Bediaga, T. Frederico and O. Lourenço, *Phys. Rev. D* **89**, 094013 (2014).
 - [3] S. Kräinkl, T. Mannel and J. Virto, arxiv:1505.04111.
 - [4] G. Grayer *et al.*, *Nucl. Phys.* **B75**, 189 (1974).
 - [5] D. Aston *et al.* (LASS Collaboration), *Nucl. Phys.* **B296**, 493 (1988).
 - [6] D. Cohen *et al.*, *Phys. Rev. D* **22**, 2595 (1980).
 - [7] W. Wang, *Int. J. Mod. Phys. A* **29**, 1430040 (2014).
 - [8] K. A. Olive *et al.* (Particle Data Group), *Chin. Phys. C* **38**, 090001 (2014).
 - [9] R. Aaij *et al.* (LHCb Collaboration), *Phys. Rev. D* **90**, 112004 (2014).
 - [10] M. Bander, D. Silverman, A. Soni, *Phys. Rev. Lett.* **43**, 242 (1979).
 - [11] I. Bediaga, I. I. Bigi, A. Gomes, G. Guerrer, J. Miranda, A. C. dos Reis, *Phys. Rev. D* **80**, 096006 (2009).
 - [12] I. Bediaga, J. Miranda, A. C. dos Reis, I. I. Bigi, A. Gomes, J. M. Otalora Goicochea, A. Veiga, *Phys. Rev. D* **86**, 036005 (2012).
 - [13] B. Bhattacharya, M. Gronau, J. L. Rosner, *Phys. Lett. B* **726**, 337 (2013).
 - [14] C. Wang, Z. H. Zhang, Z. Y. Wang, X. H. Guo, arxiv:1506.00324.
 - [15] Z. H. Zhang, R. Song, Y. M. Su, G. Lü, B. Zheng, arxiv:1505.08079.
 - [16] H. Y. Cheng and C. K. Chua, *Phys. Rev. D* **88**, 114014 (2013).
 - [17] R. E. Marshak, Riazuddin, and C. P. Ryan, *Theory of Weak Interactions in Particle Physics* (Wiley-Interscience, New York, 1969).
 - [18] G. C. Branco, L. Lavoura, J. P. Silva, *CP Violation* (Oxford University Press, New York, 1999).
 - [19] L. Wolfenstein, *Phys. Rev. D* **43**, 151 (1991).
 - [20] I. I. Bigi, A. I. Sanda, *CP Violation* (Cambridge University Press, Cambridge, England, 2009), 2nd ed.
 - [21] D. Atwood, A. Soni, *Phys. Rev. D* **58**, 036005 (1998); H.-Y. Cheng, C.-K. Chua, A. Soni, *Phys. Rev. D* **71**, 014030 (2005).
 - [22] B. Aubert *et al.* (BABAR Collaboration), *Phys. Rev. D* **72**, 072003 (2005) [Erratum-ibid. *D* **74**, 099903 (2006)]; *Phys. Rev. D* **78**, 012004 (2008).
 - [23] A. Garmash *et al.* (Belle Collaboration), *Phys. Rev. Lett.* **96**, 251803 (2006).
 - [24] N. Brambilla *et al.*, *Eur. Phys. J. C* **74**, 2981 (2014).
 - [25] U. G. Meissner and W. Wang, *Phys. Lett. B* **730**, 336 (2014).
 - [26] J. R. Pelaez, F. J. Ynduráin, *Phys. Rev. D* **71**, 074016 (2005).
 - [27] E. M. Aitala *et al.* (E791 Collaboration), *Phys. Rev. Lett.* **86**, 765 (2001).
 - [28] P. C. Magalhães, M. R. Robilotta, K. S. F. F. Guimarães, T. Frederico, W. de Paula, I. Bediaga, A. C. dos Reis, C. M. Maekawa, and G. R. S. Zarnauskas, *Phys. Rev. D* **84**, 094001 (2011).
 - [29] K. S. F. F. Guimarães, O. Lourenço, W. de Paula, T. Frederico and A. C. dos Reis, *J. High Energy Phys.* **08**, 135 (2014).
 - [30] T. Frederico, K. S. F. F. Guimarães, O. Lourenço, W. de Paula, I. Bediaga, and A. C. dos Reis, *Few Body Syst.* **55**, 441 (2014).